

N 70 35668

CR 102798

MULTI-SPECIE CONDENSATION
IN EXPANDING FLOWS

June 1970

Contract NAS8-30176

CASE FILE
COPY

Lockheed

HUNTSVILLE RESEARCH & ENGINEERING CENTER

LOCKHEED MISSILES & SPACE COMPANY

A GROUP DIVISION OF LOCKHEED AIRCRAFT CORPORATION

HUNTSVILLE, ALABAMA

LOCKHEED MISSILES & SPACE COMPANY
HUNTSVILLE RESEARCH & ENGINEERING CENTER
HUNTSVILLE RESEARCH PARK
4800 BRADFORD DRIVE, HUNTSVILLE, ALABAMA

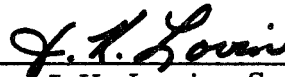
MULTI-SPECIE CONDENSATION
IN EXPANDING FLOWS

June 1970

Contract NAS8-30176

by
J. Haukohl
L. W. Spradley

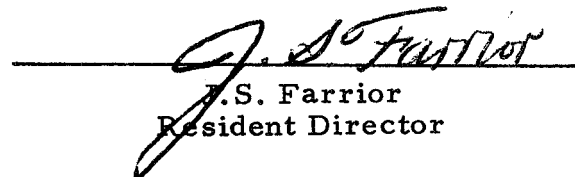
APPROVED:



J.K. Lovin, Supervisor
Thermal Environment Section



G.D. Reny, Manager
Aeromechanics Department



J.S. Farrior
Resident Director

FOREWORD

This document presents the results of work performed by Lockheed Missiles & Space Company, Huntsville Research & Engineering Center for the Aero-Astroynamics Laboratory of Marshall Space Flight Center, Huntsville, Alabama. The principal NASA technical monitors for this study were Mr. H. B. Wilson, Jr., Mr. J. L. Sims and Mr. D. Seymour.

This document is the final report on Contract NAS8-30176, "An Analytic Investigation of Jet Plumes in a Vacuum." It presents the results of work performed to meet the following requirements:

1. Obtain a basic understanding of the condensation process when several species are present.
2. Develop realistic mathematical models for a variety of flow condensation processes.
3. Incorporate and couple the models to existing plume and heat transfer definition methods.

ACKNOWLEDGMENTS

The authors are grateful for the many helpful suggestions given by J. L. Sims and D. Seymour, the principal NASA technical supervisors for this contract. Sincere acknowledgment is also given to M. M. Penny of the propulsion section of Lockheed/Huntsville for the development of the axisymmetric flow and characteristic equations presented in Appendix C of this report.

SUMMARY

A multi-specie condensation theory, which uses the classical homogeneous nucleation concept and a newly developed heterogeneous droplet growth model, was developed and coupled to nozzle and plume flow field computer programs. A one-dimensional flow/multi-specie condensation program was developed so that knowledge could be gained to develop an axisymmetric solution. Applications of the program include a single specie system, a one condensable specie in a carrier gas and several condensable species in a carrier gas.

Equations describing the nucleation phenomenon were derived following the classical approach for each specie in the system, using the specie properties at the flow temperature and its partial pressure found by Dalton's law. The equations describing the droplet growth (taking place after nucleation has created a droplet of sufficient size) were derived by allowing molecules of any specie which has crossed its vapor pressure curve to stick onto droplets present in the system. Mass accumulation is accounted for through a mass growth equation.

The relationship between flow and condensate is through the mixture density which is used in the continuity and momentum equations. Mixture density is a function of mass fraction of condensate and gas density. This relationship allows the equation of state to be solved in terms of either gas density or mixture density. The energy exchange between the gas and condensate is accounted for in the flow energy equation through the mass fraction of condensate latent heat term and the thermal energy difference between condensate and flow.

A set of equations has been derived which govern the flow of a gas-condensable vapor mixture for the axisymmetric problem to be solved by the method-of-characteristics. The equations represent a set of coupled relations between the condensed species and the gaseous mixture in that the mass transfer from the gaseous phase is considered and the energy equation accounts for the heat gain due to the phase change phenomenon.

Results are presented for several flow/condensation problems. Solutions using the present analysis are compared to existing theoretical results for a single-specie system. The comparisons are in good agreement within the assumptions which are made. Present solutions for a condensable specie in a carrier gas are compared to experimental measurements. The static pressure profiles are compared and found to be in excellent agreement. Results for a two-condensable specie system are also presented. Solutions indicate that the present model produces correct trends for the heterogeneous case. No test results are available for comparison. The present theory indicates that multi-specie condensation has a significant effect on the expansion of vapors into a vacuum environment.

CONTENTS

Section	Page
FOREWORD	ii
SUMMARY	iii
NOMENCLATURE	vi
1 INTRODUCTION	1
2 MULTI-SPECIE CONDENSATION THEORY	2
2.1 Nucleation Process	2
2.2 Heterogeneous Droplet Growth	4
3 ONE-DIMENSIONAL CONDENSING FLOW	9
4 DISCUSSION AND RESULTS	13
5 CONCLUSIONS AND RECOMMENDATIONS	23
5.1 Conclusions	23
5.2 Recommendations	24
6 REFERENCES	25
APPENDIXES:	
A: User's Manual – One-Dimensional Flow/ Multi-Specie Condensation Program	A-1
B: Development of Nucleation Rate and Drop Growth Equations for Multiple Species	B-1
C: Development of Axisymmetric/Condensation Flow and Characteristic Equations	C-1

NOMENCLATURE

A	cross-sectional area of nozzle
C_p	specific heat at constant pressure
g	number of molecules in a droplet cluster
G	Gibbs free energy
h	distance between two molecules
h_{fg}	specific enthalpy of vaporization
H	total enthalpy
I	inertia of molecule cluster
J	nucleation rate
k	Boltzmann constant
K	number of condensable species
m	molecular weight
M	mass in Section 2, Mach number in Section 3
N	number of molecules
N_A	Avogadro's number
N(g)	Boltzmann distribution
P	pressure
r	droplet radius in Section 2, axisymmetric radius in Section 3
R	gas constant
\mathcal{R}	Universal gas constant
S	entropy
S(g)	surface area of g sized drops
t	time

T	temperature
U	freestream velocity
U_{fD}	internal energy
X	axial distance of nozzle centerline
I, II	nucleation combination possibilities of two species

Greek

α	thermal accommodation coefficient (otherwise defined in Appendix C)
β	rate at which molecules strike unit surface area (otherwise defined in Appendix C)
Δ	symbol denoting change or increment
γ	ratio of specific heats
$\gamma(g)$	rate at which molecules leave unit surface area
η	quasi-equilibrium droplet density distribution
ξ	condensation coefficient (mass accommodation)
$\bar{\mu}$	chemical potential
μ	mass fraction
\mathcal{N}	mole fraction
ρ	density
σ	droplet surface tension
Ω	cluster molecular volume in gaseous standard state

Subscripts

a	surface
b	bulk phase
D	droplet
E	energy
i	specie

g	gas
I	condensate (homogeneous or heterogeneous)
∞	flat film equilibrium condition
j	specific droplet or composition
L	liquid
m	number of quasi-equilibrium volume elements
o	total or stagnation
r	rotation
ref	reflected
s	separation
t	translational
Superscript	
*	symbol denoting "critical size"; denotes throat conditions in Section 3

Section 1

INTRODUCTION

A condensation phenomenon may result when a compressible vapor in a jet plume is expanded into a vacuum environment. During the evolution of condensate within an expansion process, the latent heat of the vapor is released, changing the vapor from an unsaturated state to a supersaturated state. This results in a significant change in the flow properties, which, in turn, determine jet plume shapes necessary in nozzle design and plume impingement studies. Recent interest has also centered on contamination in a vacuum environment in which the condensation mechanism aids in describing the contamination source and contamination rate.

Most experimental and theoretical work which has been done on the condensation phenomenon has been with pure vapors (Refs. 1 through 26). A realistic application of the problem, however, must include the effects of a multiple-specie vapor. This study extends existing theories of condensation in expanding flow to account for multiple species. The condensation model has been coded into a One-Dimensional Flow/Multiple-Specie Condensation Program utilizing FORTRAN IV language. Equations for axisymmetric condensing flow have also been derived. The basic theory behind multiple specie condensation and its occurrence in expanding flows is the subject of the main portion of this report. The one-dimensional flow equations were rederived to account for multiple specie effects. Energy effects from the transient flow properties were also considered. Results obtained for single specie systems and a multi-specie system are presented in Section 4. A user's guide for the computer program is presented in Appendix A and a complete derivation of the governing equations is described in Appendix B. The condensation theory advanced in this study has been coupled to the axisymmetric flow equations for solution by the method of characteristics (Appendix C). Finally, conclusions are drawn from this study and recommendations for future work are presented.

Section 2

MULTI-SPECIE CONDENSATION THEORY

Condensation is essentially a bimolecular reaction. Gas molecules collide with the surface of a condensed phase already in existence. These surfaces are assumed to be spherical-shape nuclei created by the nucleation process. The accumulation of gas molecules onto the nuclei are descriptive of droplet growth. Condensation theory is therefore described by two distinct processes: (1) nucleation, and (2) droplet growth. Section 2.1 discusses the nucleation theory and Section 2.2, heterogeneous droplet growth.

2.1 NUCLEATION PROCESS

The approach used to describe the nucleation process of different gaseous components is based upon the classical nucleation theory advanced by Frenkel (Ref. 1). Appendix B presents a detailed derivation of these homogeneous nucleation rate equations. It is assumed the condensation phenomenon is described by spontaneously formed nuclei onto which supersaturated vapor condenses after the nuclei have attained a certain size (termed critical size). Frenkel (Ref. 1) develops the concept of homogeneous nucleation by first assuming a Boltzmann distribution for the distribution of clusters of vapor molecules. This results in an expression defining the number of nuclei formed per unit time and volume. The expression, given by

$$N(g) = N_o e^{(-\Delta G/kT)} \quad (1)$$

makes use of the change in Gibbs free energy, ΔG , which, in the classical approach, consists of the reversible work effect of condensation to the bulk phase and the work required to produce a free surface. Assuming homogeneous nucleation only of all species, Eq. (1) becomes

$$N_i(g) = N_{o_i} e^{(g_i \ln(P_i/P_{\infty_i}) - 4\pi r_i^2 \sigma_i / kT)} \quad (2)$$

The maximum Gibbs free energy change is found by taking the derivative of the energy term with respect to g_i , the number of specie i molecules, and setting the result equal to zero. By substituting appropriate terms the Kelvin-Helmholtz expression is derived which describes the equilibrium conditions of a liquid drop with its vapor phase.

$$\ln\left(\frac{P_i}{P_{\infty_i}}\right) = \frac{2m_i \sigma_i}{\rho_{L_i} k T N_A r_i^*} \quad (3)$$

Equation (3) is the definition of the critical drop radius, r_i^* , which gives the droplet an equal probability to condense or evaporate.

This analysis assumes, as does Griffin (Ref. 2), that since an expansion process reduces the specie partial pressure in an infinitesimal amount of time, r_i^* is defined as the initial droplet size of specie i .

With use of kinetic theory and a few simplifying assumptions set forth in Appendix B, one arrives at the classical nucleation rate equation.

$$J_i = \left(\frac{P_i}{kT}\right)^2 \frac{m_i}{\rho_{L_i}} \left(\frac{2\sigma_i}{\pi m_i}\right)^{1/2} e^{\left(\frac{-4\pi \sigma_i r_i^{*2}}{3kT}\right)} \quad (4)$$

The nucleation rate equation is critically dependent upon the value of liquid surface tension. An argument used by Duff (Ref. 3), Sivier (Ref. 4) and others is that effects of curvature are not properly accounted for by the linear variation of temperature (used by Griffin). Tolman (Ref. 8) approximated the effect by

$$\sigma_i = \frac{\sigma_{i\infty}}{1 + \frac{D_i}{r_i^*}} \quad (5)$$

in which $\sigma_{i\infty}$ is the surface tension of an infinite plane surface of specie i and D_i is the Tolman constant of specie i , a dimension related to the inter-molecular distance in the liquid drop. Since surface tension is used only in the nucleation process of the condensation phenomena, the Tolman constant D can only influence the physical location and slope of the nucleation curve with respect to nozzle distance.

2.2 HETEROGENEOUS DROPLET GROWTH

When a droplet reaches critical size from the homogeneous nucleation phenomenon, continued molecular collisions cause droplet growth. A droplet of critical size has the equal probability of condensing and evaporating. However, in an expansion process, the specie vapor pressure continues to decrease, forcing condensation to become dominant over evaporation. The term heterogeneous droplet growth indicates that the growth equations developed in Appendix B allow molecules of different species to "stick" to droplets present in the system. Prior to this occurrence, however, the specie partial pressure must cross into the liquid or solid phase of its vapor pressure curve, thereby establishing itself as a potential condensable. A potential condensable becomes a condensable when critical-size nuclei or droplets are present, or when it grows onto droplets already present in the system.

All droplets formed in the same quasi-static volume element have the same growth. Therefore, since a new set of droplets is formed in each volume element and the new size of the droplets formed in the preceding volume element must be known, each droplet type must be separately distinguished and subscripted by j in the equation development. The growth rate of any droplet type j may be written from the conservation of mass as

$$\left. \frac{dr}{dt} \right|_j = \sum_i^n \frac{\xi_i}{\rho_{L_i} (2\pi R_i)^{1/2}} \left[\beta_i - \beta_{D_j} \right] \quad (6)$$

where $\beta_i = \frac{P_i}{T^{1/2}}$ and $\beta_{D_j} = \frac{P_{D_j}}{T_{D_j}^{1/2}}$.

The condensable specie i condenses at the β_i properties and evaporates at the β_{D_j} properties. The energy transfer to the droplets from impinging and vaporizing molecules leaves the droplet temperature higher than the temperature of the surrounding environment. The temperature difference between the droplets and surrounding vapor allows droplet growth.

The conservation of energy based upon the change of droplet internal energy due to droplet growth is

$$\begin{aligned} & \left. \frac{r_j \rho_{L_j} C_{p_j}}{3} \frac{dT_{D_j}}{dt} \right|_j + \rho_{L_j} \left(\frac{\gamma_j}{\gamma_j - 1} R_{I_j} T_{D_j} - h_{fgI_j} \right) \frac{dr}{dt} \\ & - \sum_i^n \left(\frac{\beta_i (2 R_i T)}{(2 \pi R_i)^{1/2}} - (1 - \xi_i) \frac{\beta_i (2 R_i)}{(2 \pi R_i)^{1/2}} \left[T + \alpha_j (T_{D_j} - T) \right] \right. \\ & \quad \left. - \frac{\xi_i \beta_{D_j} (2 R_i T_{D_j})}{(2 \pi R_i)^{1/2}} \right) = 0 \end{aligned} \quad (7)$$

With use of the perfect gas assumption, the definition of droplet growth, and algebraic manipulations, the final form* of the energy equation is

$$\begin{aligned} & \left. \frac{r_j \rho_{L_j} C_{p_j}}{3} \frac{dT_{D_j}}{dt} \right|_j + \sum_i^n \left(\xi_i \beta_{D_j} \sqrt{\frac{2 R_i}{\pi}} + (1 - \xi_i) \beta_i \sqrt{\frac{2 R_i}{\pi}} \alpha_j \right) T_{D_j} \\ & - \sum_i^n \left\{ \xi_i \beta_i T \sqrt{\frac{2 R_i}{\pi}} + (1 - \xi_i) \beta_i \sqrt{\frac{2 R_i}{\pi}} \alpha_j T \right. \\ & \quad \left. + \frac{\xi_i}{\sqrt{2 \pi R_i}} (\beta_i - \beta_{D_j}) \left(\frac{\gamma_j}{\gamma_j - 1} \right) (\lambda_j - 1) R_{I_j} T_{D_j} \right\} = 0 \end{aligned} \quad (8)$$

* The first term of Eq. (8) is dropped in the computer solution (see Appendix B for discussion).

Equation (8) is used to obtain the droplet temperature for those drops which have become larger than critical size. Griffin (Ref. 2) defines all droplet temperatures as the saturation temperature at the specie vapor pressure. Experience shows that after nucleation has been completed, the droplet temperatures converge to the flow temperature. The newly nucleated droplets of critical size are defined by Duff (Ref. 3) and Griffin (Ref. 2) to occur at the saturation temperature. Application of Eq. (8) to a droplet, one quasistatic volume element after it has reached critical size, yields a droplet temperature somewhere between saturation and freestream value. This indicates that an argument exists against defining the temperature of a newly formed droplet as its saturation value.

Obviously, during the nucleation process, the buildup of specie molecules constitutes a buildup of energy, raising the nuclei temperature above that of the freestream. A smaller temperature discontinuity exists between the newly formed droplet and its first droplet temperature, based upon growth, by setting the temperature of the newly formed droplet equal to the flow temperature, rather than at the saturation temperature at the specie vapor pressure. Therefore, in the theory of this analysis the flow temperature is used to define the newly nucleated droplet temperature. Prediction of the condensation phenomenon is not affected by this assumption. For this reason, nucleation properties are calculated at the flow temperature and droplet properties are calculated at the droplet temperature.

Coupling the condensation to the flow requires that the mass fraction of condensate be described for each specie in each quasistatically defined volume. The equation describing the mass of the newly formed droplets of specie i in each volume element is

$$M_{ND_i}(X_m) = J_i(X_m) A(X_m) \left[\frac{dX_m}{u} \right] dX_m \rho_{L_i} \left(\frac{4}{3} \pi r_i^{*3} \right) \quad (9)$$

Another mass contribution to the condensed phase is that mass obtained through droplet growth. From kinetic theory, the mass growth rate of specie i from volume element X_{m-1} to X_m is

$$\left. \frac{dM_i}{dt} \right|_{X_{m-1}}^{X_m} = \sum_{j=1}^{KN} \frac{\xi_i S_j}{(2\pi R_i)^{1/2}} \left[\frac{P_i}{T^{1/2}} - \frac{P_{D_j}}{T_{D_j}^{1/2}} \right] ND_j \quad (10)$$

where KN is the number of types of drops in the volume element and ND_j is the number of drops of type j . (11)

S_j describes the surface area of any droplet j . The expression for S_j is given by

$$S_j = 4\pi \left[r_j \Big|_{X_{m-1}}^{X_m} + \int_{X_{m-1}}^{X_m} \frac{ND_j}{u} \sum_i^{KN} \frac{\xi_i}{\rho_{LI_j} (2\pi R_i)^{1/2}} \left[\frac{P_i}{T^{1/2}} - \frac{P_{D_j}}{T_{D_j}^{1/2}} \right] dX_m \right]^2 \quad (12)$$

The total condensed mass of specie i may be mathematically defined as

$$M_i(X_m) = M_{ND_i}(X_m) + M_i(X_{m-1}) + \left. \frac{dM_i}{dt} \right|_{X_{m-1}}^{X_m} \frac{dX_m}{u} \quad (13)$$

The first term of Eq. (13) defines the mass of the new droplets formed in the volume element at X_m , the second term is the total condensed mass in the volume element at X_{m-1} and the last term defines the mass growth of the droplets from X_{m-1} to X_m . The specie i mass fraction of condensate is therefore equated to

$$\mu_i = \frac{M_i(X_m)}{\rho A d X_m}$$

(14)

The total mass fraction of condensate is obtained by summation μ_i over all i . The total mass fraction of condensate along with ρ , the mixture density, is used to couple condensation to the flow equations.

The droplet model used in this analysis is one termed as a "homogenous mixture" model. This means that mass dependent properties mix instantaneously into a droplet. The added condensate is dependent upon the specie gas mass available to condense.

Section 3

ONE-DIMENSIONAL CONDENSING FLOW

A one-dimensional flow analysis linked with condensation was performed for two reasons: (1) the one-dimensional flow equations are easily linked to condensation and a computer program describing the phenomenon will represent an easy tool to define multi-specie condensation/flow problems which will be encountered in developing an axisymmetric solution; (2) several one-dimensional flow/homogeneous condensation techniques, by Duff (Ref. 3), Griffin (Ref. 2) and Roberts (Ref. 5) have been presented along with supporting data. This allows the multi-specie condensation theory to be checked out both for homogeneous condensation and for a single condensable specie in a carrier gas.

The one-dimensional flow mechanism describing condensation is one of isentropic flow until the onset of condensation and then condensing flow thereafter. The onset of condensation as defined in this analysis is dependent upon three conditions: (1) the expansion isentrope must cross into the liquid or solid state of a specie vapor pressure curve, thereby establishing a potential condensable; (2) the nucleation theory must experience enough specie molecular collisions to create a critical-sized droplet; and (3) enough droplets must be formed so that the expansion process deviates from the isentropic expansion.

The assumptions for the flow processes used in this analysis follow the work of Griffin (Ref. 2) with the exception that a temperature difference between phases is allowed in the present work. These assumptions are summarized as follows:

- Mass flow is conserved.
- Flow is one-dimensional and steady state.
- The condensed phase volume is negligible by comparison to the total volume.

- The nozzle is frictionless with no heat transfer across the wall.
- The condensed phase is uniformly distributed throughout the quasistatic volume element and has no velocity lag with the gas.

The one-dimensional system of equations describing the flow prior to the intersection of the specie vapor pressure curve is described by the isentropes relations.

$$P = P_o \left(\frac{T}{T_o} \right)^{\frac{\gamma}{\gamma-1}} \quad (15)$$

$$M = \left[\frac{2}{\gamma-1} \left(\frac{T_o}{T} - 1 \right) \right]^{1/2} \quad (16)$$

$$\rho = \rho_o \left[1 + \frac{\gamma-1}{2} M^2 \right]^{-\frac{1}{\gamma-1}} \quad (17)$$

$$A = \frac{A^*}{M} \left[\frac{2}{\gamma+1} \left(1 + \frac{\gamma-1}{2} M^2 \right) \right]^{\frac{\gamma+1}{2(\gamma-1)}} \quad (18)$$

$$U = \left[2 C_p (T_o - T) \right]^{1/2} \quad (19)$$

Equations (15) through (19) are evaluated for given P_o , T_o , ρ_o , γ , C_p and A^* for any value of T . The nozzle geometry is assumed to be known a priori.

The saturation crossing point is found by an iterative solution of a curve fit equation for the vapor pressure given by

$$T_{sat} = \frac{C_1}{C_2 - \log_e P_{sat}} \quad (20)$$

(where C_1 , C_2 are curve-fit coefficients for the specie being considered) and

the isentropic relation

$$P_{\text{sat}} = P_o \left(\frac{T_{\text{sat}}}{T_o} \right)^{\frac{\gamma}{\gamma-1}} \quad (21)$$

After the saturation crossing point has been reached, the one-dimensional flow condensation equations are used to describe the system. The equation of state and equations of conservation of mass, momentum and energy can be described in terms of the mixture density discussed by Stever (Ref. 6). The mixture density of the system can be written as

$$\frac{1}{\rho_{\text{mix}}} = \frac{1-\mu}{\rho_{\text{gas}}} + \frac{\mu}{\rho_{\text{Liq}}} \quad (22)$$

The last term of Eq. (22) is dropped since the assumption was made that the condensed phase volume is negligible in comparison with the total volume.

In addition, the gaseous mixture molecular weight m reduces as more gas undergoes a phase change. The one-dimensional flow equations linked with condensation are therefore written as:

Continuity Equation

$$\frac{d\rho}{\rho} + \frac{dU}{U} + \frac{dA}{A} = 0 \quad (23)$$

Momentum Equation

$$\frac{dP}{P} = \frac{-U}{(1-\mu)} \frac{dU}{\frac{R}{m} T} \quad (24)$$

Equation of State

$$\frac{dP}{P} = \frac{d\rho}{\rho} + \frac{dT}{T} - \frac{d\mu}{(1-\mu)} - \frac{dm}{m} \quad (25)$$

where ρ is the mixture density and m is the molecular weight based on the gaseous mixture mole fraction.

Energy Equation

$$U dU + C_{pg} dT - \sum_{i=1}^N \left[L_i + C_{pL_i} (T - T_D) \right] d\mu_i = 0 \quad (26)$$

where C_{pg} is the specific heat of the initial gas mixture, C_{pL_i} is the specific heat of specie i liquid and T_D is an average droplet temperature.

Equations (23) through (26) describe the flow of a one-dimensional expansion process including condensation.

Section 4

DISCUSSION AND RESULTS

This section is to establish the validity of the theory advanced herein by comparing theory with experiment for a selected set of data and to present results for a multi-specie system. The data were taken from experiments which included a homogeneous nitrogen expansion in a 25 cm nozzle and a mixture of water vapor and air in a 30 cm nozzle. No data were available to compare the multiple specie condensation theory; however, results shown for the two-specie condensable system demonstrate correct trends.

Data for the homogeneous gas expansion of 100 percent nitrogen were taken from tables presented by Griffin (Ref. 2). The experiment was performed by Willmarth and Nagamatsu (Ref. 7). Exact comparison of theory with data was not attempted as the expansion process in the theory was assumed at a constant specific heat ratio expansion. The computer program is not restricted to this assumption however. It was made in the nitrogen expansion case as the variable specific heat ratio assumption was not necessary for the remaining checkout cases. In any event, the results presented for the homogeneous nitrogen expansion serve to illustrate correct trends of thermodynamic and condensation theory parameters.

Figure 1 is a plot of static pressure to stagnation pressure ratio versus nozzle distance from the throat. The results show that the presence of condensate increases static pressure. This is expected as the density of the gas-liquid mixture is higher than its pure gas value. The low pressure ratio at which condensation occurred is an indication of the low vapor pressure of nitrogen at which the expansion isentrope crossed.

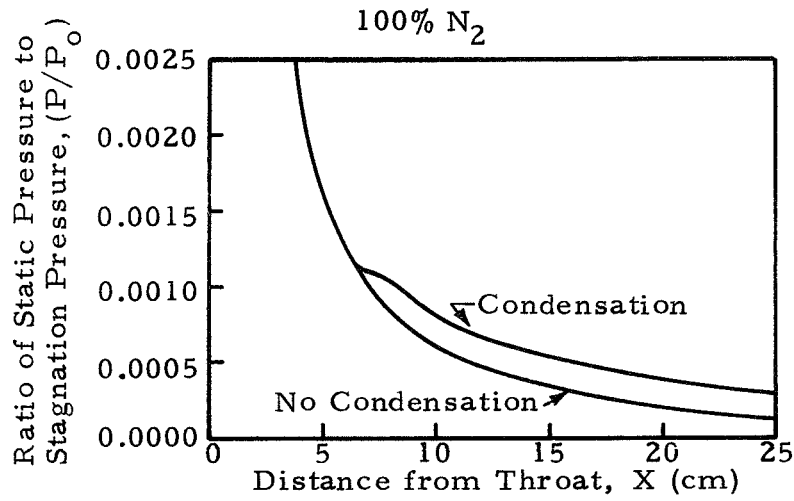


Fig. 1 - Theoretical Pressure Ratio Distribution Along Nozzle Wall for a 100% Nitrogen Gas Expansion

Figure 2 is a plot of the ratio of local static temperature to stagnation temperature versus nozzle distance from the throat. This figure shows that the condensation mechanism brings on a thermal energy increase. This imbalance in a total energy analysis is made up by a kinetic energy loss as velocity reduces with the presence of condensate.

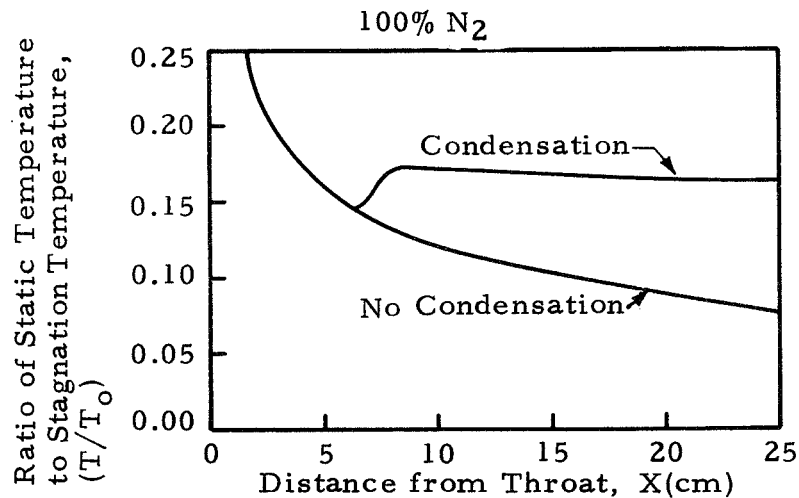


Fig. 2 - Temperature Ratio Increase with Condensation Compared to 100% Nitrogen Gas Expansion without Condensation

Figure 3 is a plot of static pressure versus flow temperature for the nitrogen gas expansion. After the isentrope crosses the nitrogen vapor pressure curve, condensation occurs, causing the flow temperature to increase drastically. After the thermal energy exchange has transpired, the expansion process is noted to follow the nitrogen vapor pressure curve.

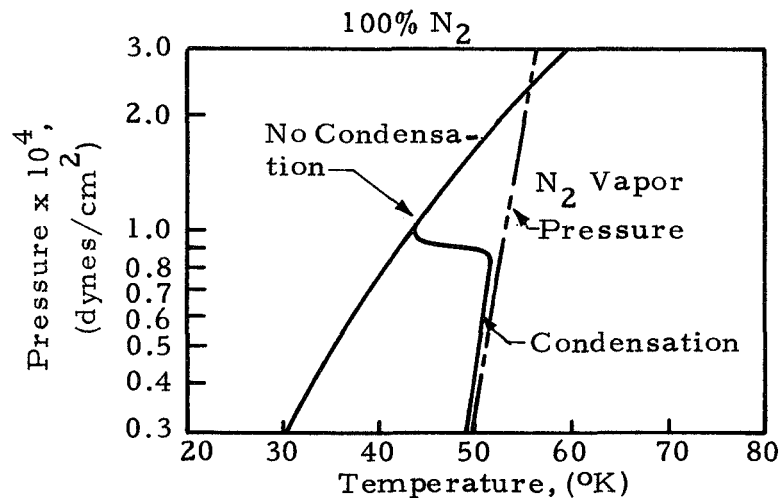


Fig. 3 - Nitrogen Expansion Condensation History of Pressure vs Temperature

The results of Fig. 4 demonstrate the critical radius criteria and the nucleation curve. Nucleation is seen to occur over a very short distance in the nozzle. Droplets are formed only during the nucleation process and are considered droplets only when they have reached critical size, r^* . The critical radius plot is meaningful only during the nucleation process. Nitrogen results show that 0.5×10^{-7} cm is an average size for droplets to occur in the theory.

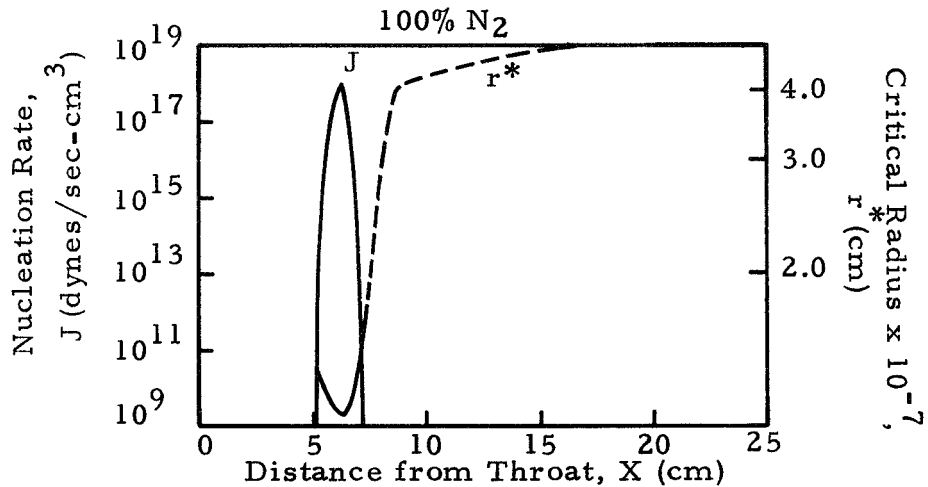


Fig. 4 - Nucleation Rate and Critical Radius as a Function of Distance from Throat

Figure 5, the final plot for the 100 percent nitrogen gas expansion, shows mass fraction of condensate as a function of nozzle distance. The steepest gradient in the curve occurs at the same nozzle station as the nucleation curve of Fig. 4. Results of the present theory are not to be compared quantitatively to the Griffin theory as thermodynamic conditions for the cases were different. Both cases do show, however, that about 10 percent of the nitrogen gas changes into the liquid phase.

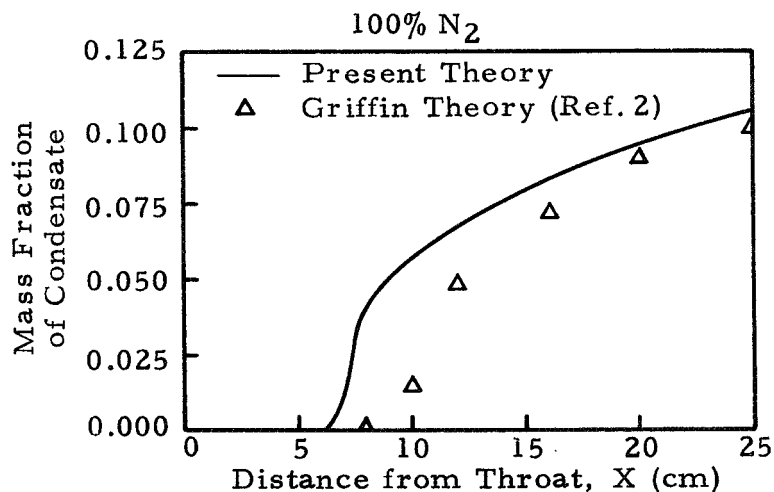


Fig. 5 - Trends of Mass Fraction of Condensate as a Function of Nozzle Position for Present Theory and Griffin Theory (Ref. 2)

The second checkout case investigated was that of a mixture of $1\frac{1}{2}$ percent water vapor and $98\frac{1}{2}$ percent air. Although the purpose of Roberts (Ref. 5) was to measure droplet size using light scattering techniques, he obtained static pressure data within the region of condensation along the 30 cm nozzle. These results are shown in Fig. 6. Shown on the graph is a plot of the ratio of static pressure to stagnation pressure versus distance from the throat. The lower curve is the isentrope of the expansion process. Theory shows excellent agreement with data in the influence of condensation on static pressure.

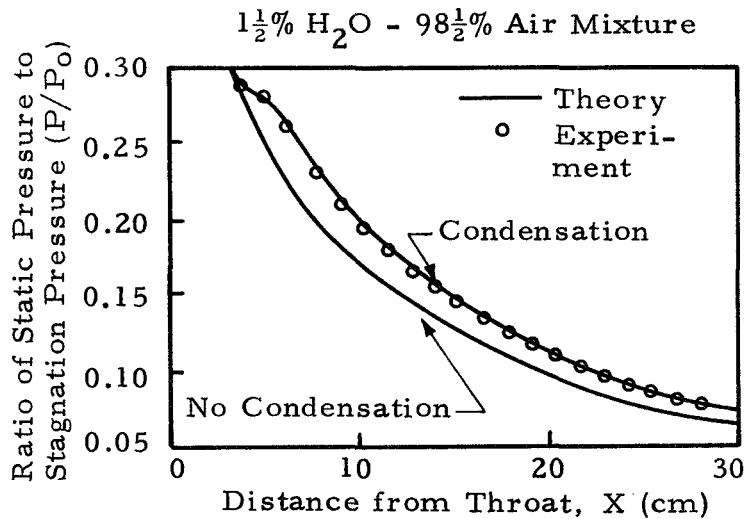


Fig. 6 - Comparison of Multi-Specie Condensation Theory with Experimental Data Published by Roberts (Ref. 5)

The curves presented in Fig. 7 represent the ratio of static to stagnation temperature as a function of distance from the throat for both the isentropic expansion and the expansion with condensation. Results show a significant increase in temperature for a small mass fraction of potential condensable ($1\frac{1}{2}$ percent water).

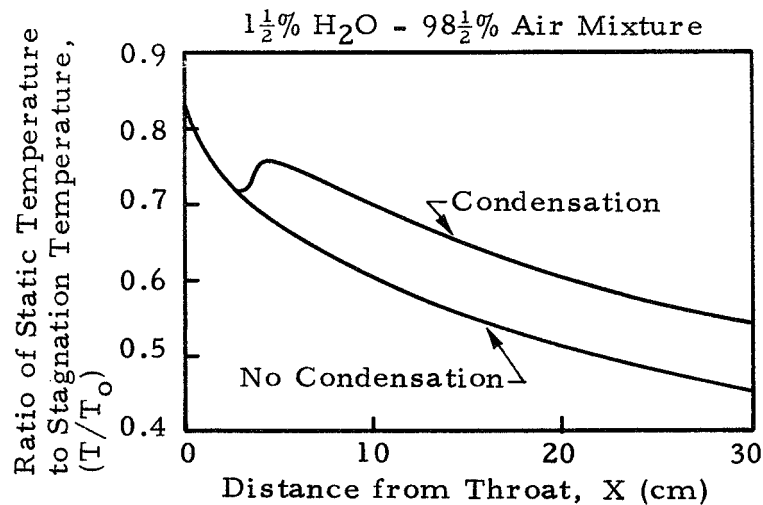


Fig. 7 - Temperature Ratio Increase with Condensation Compared to Water-Vapor-Air Mixture Expansion without Condensation

Figure 8 shows the expansion process of the water vapor-air mixture in the pressure-temperature plane. The expansion including condensation shows a rise in pressure, analogous to an expansion process in a diffuser.

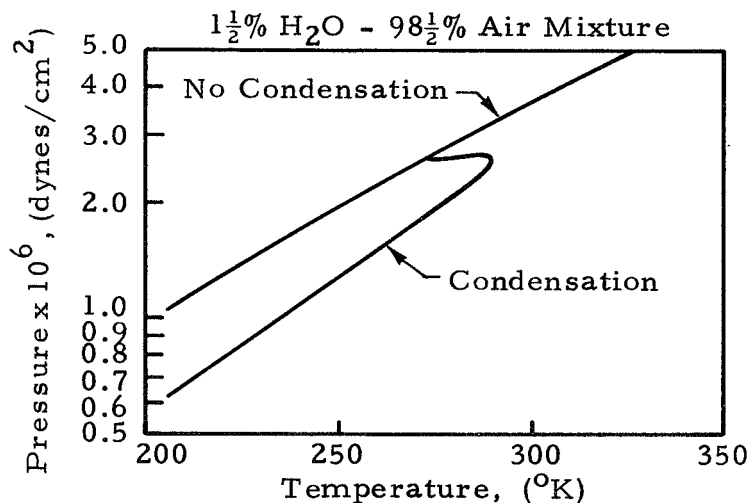


Fig. 8 - Pressure Versus Temperature Plot of Water Vapor-Air Mixture for Isentrope and Expansion with Condensation

The curves presented in Fig. 9 show the nucleation rate and critical radius calculation of water in the water vapor-air mixture. The nucleation of droplets is seen to occur over a 2 cm nozzle distance. This sudden presence of liquid in the flow helps to explain the sudden pressure and temperature changes of Fig. 8. The critical radius curve calculation, meaningful only during nucleation, is a minimum at the maximum nucleation rate from application of the kinetic theory.

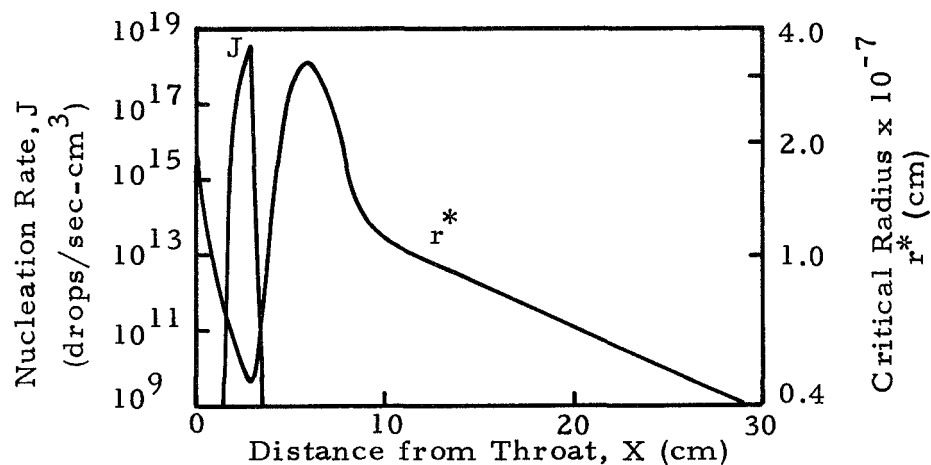


Fig. 9 - Nucleation Rate and Critical Radius Versus Distance from Throat for Water Vapor-Air Mixture

Figure 10 is a curve depicting the amount of water condensate present at any nozzle station. Correlation of nozzle positions of the nucleation curve of Fig. 9 and the results in Fig. 10 show that only about 30 percent of condensate present in the system was formed from nucleation while 70 percent was formed from droplet growth.

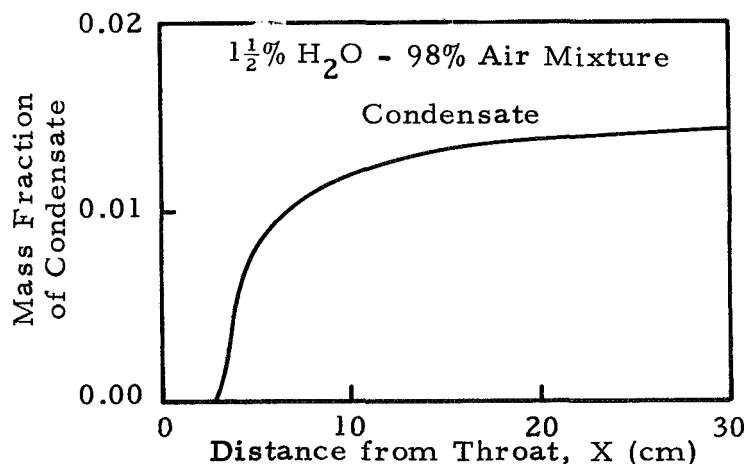


Fig. 10 - Mass Fraction of Condensate as a Function of Nozzle Position for Water in the Water Vapor-Air Mixture

The next set of curves shows results of the multiple condensing species theory. The results were obtained from a mixture of 50 percent carbon dioxide and 50 percent fictitious gas. The fictitious gas was created so that condensation effects could be studied for large amounts of potential condensable gases (therefore the 50 percent - 50 percent by weight mixture) with almost identical vapor pressure curves (5°K apart). The nozzle was an 11-degree expansion cone with a throat area of 0.0025 cm^2 .

The result shown in Fig. 11 is the pressure-temperature plane expansion compared to the isentropic expansion. The temperature rise is due to condensation since the latent heat of the vapor is given up to the flow during the phase change.

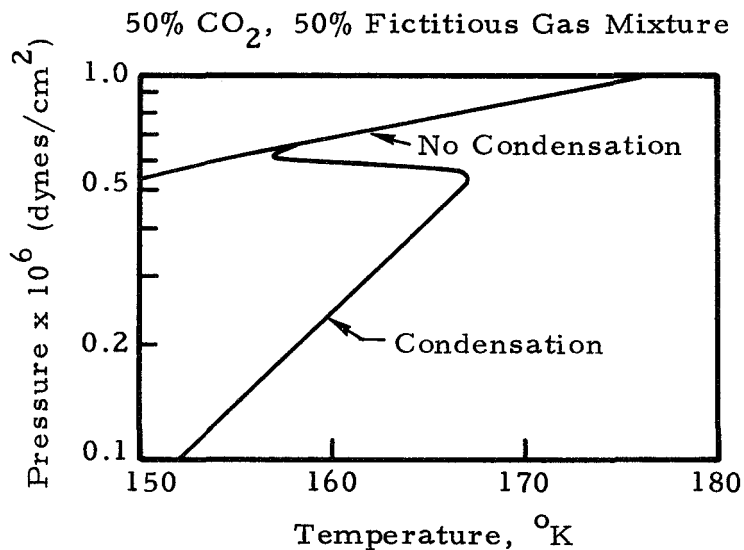


Fig. 11 - Pressure Versus Temperature for Two Condensable Species System

Figure 12 is a plot of nucleation rate as a function of nozzle position from the throat for both the carbon dioxide and fictitious gas. The nucleation rate of the second condensable species (fictitious species) is six orders of magnitude lower than the first condensable species (CO₂). The nucleation peak, however, occurs at the same time.

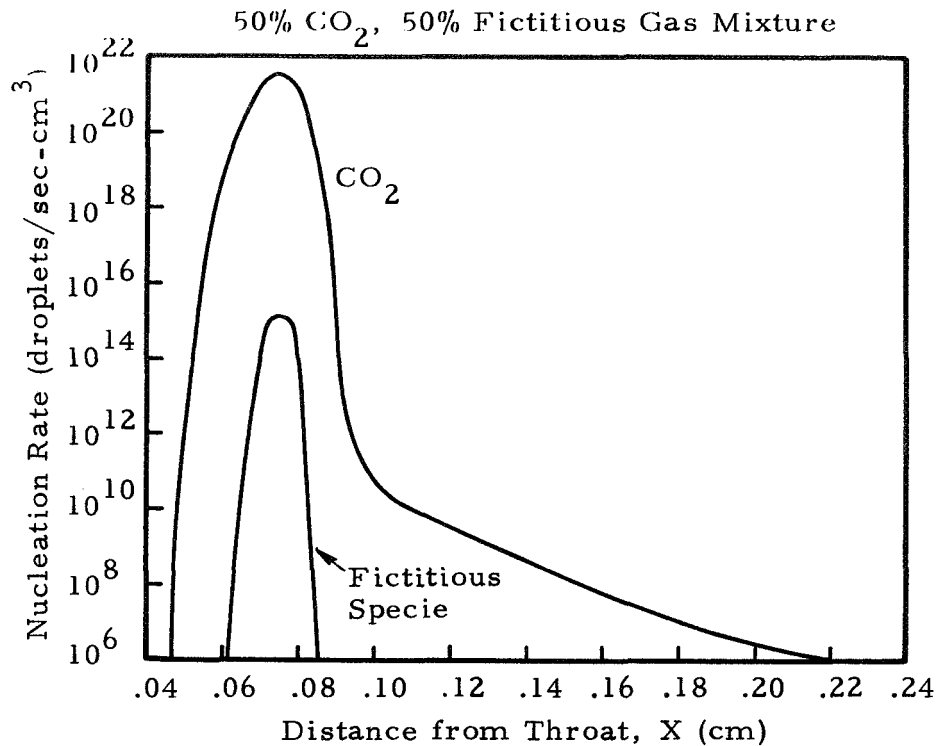


Fig. 12 - Nucleation Rate of Carbon Dioxide and Fictitious Gas as a Function of Distance from Throat

The mass fraction of condensate along with droplet density is plotted as a function of distance from the throat in Fig. 13. The reasonably small flow temperature increase shown in Fig. 11 is substantiated by the slow increase in mass fraction of condensate. Droplet number density, on the other hand, reaches its maximum almost instantaneously. This is an indication that most of the condensate is created through droplet growth.

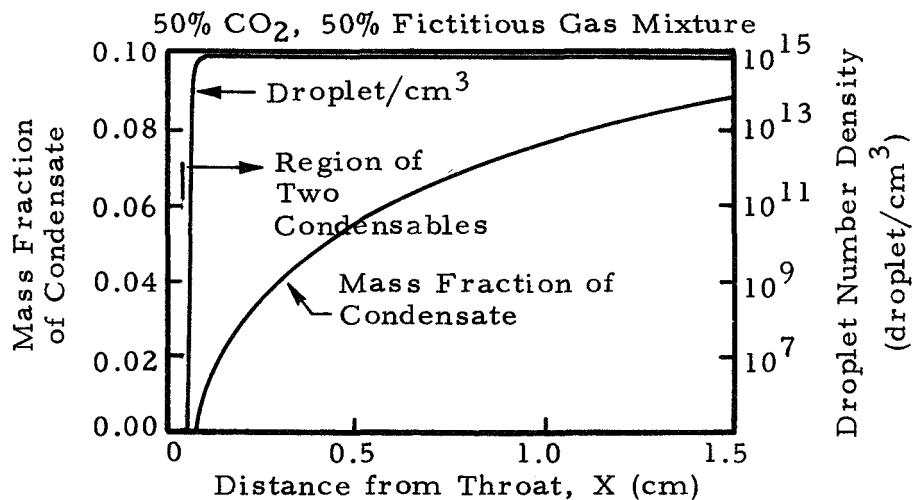


Fig. 13 - Mass Fraction of Condensate and Droplet Density versus Distance from Throat

Another checkout case for multiple condensing species was attempted. This multiple species checkout case was a mixture of 0.4 percent water vapor, 4.6 percent ammonia and 95 percent air. The expansion nozzle was "Nozzle I" used by Duff, (Ref. 3) in his homogeneous carbon dioxide condensation studies. The chamber temperature was 388.16°K and the chamber pressure was 0.8375×10^7 dynes/cm³. The results of this case are not presented in this report since their validity has not been established. The deviation of the expansion from the isentrope was described by a strong surge compared to single condensable results. A qualitative analysis indicates that more than just condensation is responsible for the surge. The pressure-temperature plot shows such a large jump in temperature that the saturation curve is re-crossed. This problem will require further investigation.

Section 5

CONCLUSIONS AND RECOMMENDATIONS

5.1 CONCLUSIONS

Computer results of the One-Dimensional Flow/Multi-Specie Condensation Program have compared well with existing data for the homogeneous nitrogen expansion and the water vapor-air mixture. Homogeneous gas expansions certainly apply to the program as the equations in the theory reduce to those of Duff (Ref. 3) for the single specie case. The excellent comparison of static pressure in the $1\frac{1}{2}$ percent water vapor and $98\frac{1}{2}$ percent air mixture of Roberts (Ref. 5) show the theory and the present computer program to be valid for a single condensable specie with a carrier gas.

A test program to further validate the multi-specie condensation concept was not within the scope of this contract. A literature search of test data did not uncover a suitable multi-specie test case.* One may conclude, however, that on the basis of the hypothetical example data case presented in Figs. 11 through 13 that all thermodynamic parameters behaved in the proven trends of existing data. One may further conclude that the presence of an additional condensable specie in the system causes a tremendous amount of droplet growth onto the droplets already present in the system. A consistent result with the foreign particle concept is that when particles or droplets are already present, nucleation of a new specie does not create many new droplets.

The theory, in calculating the condensation equations, also forces convergence of droplet temperature. This allows an additional heat transfer term accounting for the temperature difference between the condensate and the flow. The present analysis has shown that this term may not always be neglected when multiple species are considered.

*The work of Jaeger (Ref. 27) was investigated. The ammonia-water case was applied to the present analysis and was found not applicable as the water vapor was found to condense prior to the throat.

The equations for axisymmetric flow with condensation were derived and an effort was begun to modify the Streamline-Normal program* to include condensation.

The theory advanced herein should be instrumental in future work involving any problem in condensation for the homogeneous gas expansion, the single condensable specie in a carrier gas case and the multi-specie case. The computer program will also tell if condensation of any specie that is input will occur at all. The theory for several condensable species has yet to be proven to be correct or incorrect. Full validity of the theory must come from experiment.

5.2 RECOMMENDATIONS

The following is a summary of the tasks which should be performed in order to obtain additional insight into the condensation problem and to achieve a state-of-the-art capability in plume flowfield definition.

- Modify and checkout Streamline-Normal Method-of-Characteristics program to include the condensation model developed in this study.
- Develop a realistic approach to the problem of condensation flow across a shock.
- Investigate the effects of condensation on plume impingement heating.
- Study the applicability of the condensation theory to the problem of surface contamination due to rocket exhaust impingement.
- Validate the theory set forth in the One-Dimensional Flow/Multi-Specie Condensation computer program through an experimental program.

* The Streamline-Normal program employs an axisymmetric Method-of-Characteristics solution to the flow of a supersonic gas. However, the solution proceeds along normals to the characteristic lines rather than along the characteristic lines themselves.

Section 6

REFERENCES

1. Frenkel, J., Kinetic Theory of Liquids, Oxford University Press, London, 1946.
2. Griffin, J. L., "Digital Computer Analysis of Condensation in Highly Expanded Flows," ARL 63-206, Wright-Patterson AFB, Ohio, November 1963.
3. Duff, K. M., "Non-Equilibrium Condensation of Carbon Dioxide in Supersonic Nozzles," Report No. 84, Gas Turbine Laboratory, Massachusetts Institute of Technology, Cambridge, Mass., January 1966.
4. Sivier, K. R., "Digital Computer Studies of Condensation in Expanding One-Component Flows," ARL 65-234, Wright-Patterson AFB, Ohio, November 1965.
5. Roberts, Richard, "A Light-Scattering Investigation of Droplet Growth in Nozzle Condensation," GTL Report No. 97, Gas Turbine Laboratory, Massachusetts Institute of Technology, Cambridge, Mass., February 1969.
6. Stever, H. G., "Condensation Phenomena in High Speed Flows," from Fundamentals of Gas Dynamics, Princeton University Press, Princeton, N. J., 1958.
7. Willmarth, W. W., and H. T. Nagamatsu, "Condensation of Nitrogen in a Hypersonic Nozzle," GALCIT Hypersonic Wind Tunnel Memorandum No. 6, January 1952.
8. Tolman, R. C., "The Effect of Droplet Size on Surface Tension," J. Chem. Phys., Vol. 17, No. 3, March 1949, pp. 333-337.
9. Oswatitsch, K., Z. Angew. Math. und Mech., Vol. 22, 1942, p. 1.
10. Rutner, E., P. Goldfinger and J. P. Hirth, "Condensation and Evaporation of Solids," Proc. of the Internat. Sympos. Condensation and Evap. of Solids, Dayton, Ohio, 12-14 September 1962.
11. Stein, G. D., and P. P. Wegener, "Experiment on the Number of Particles Formed by Homogeneous Nucleation in the Vapor Phase," AD 649260, January 1967.
12. Parlange, J. Y., "Mayer's Theory of Condensation and Homogeneous Nucleation," AD 656640, July 1967.
13. Kremmer, M., and O. Okurounmu, "Condensation of Ammonia Vapor During Rapid Expansion," Report No. 79, Gas Turbine Laboratory, Massachusetts Institute of Technology, Cambridge, Mass., January 1965.

14. Hill, P.G., "Homogeneous Nucleation of Supersaturated Water Vapor in Nozzles," Report No.78, Gas Turbine Laboratory, Massachusetts Institute of Technology, Cambridge, Mass., January 1965.
15. Lothe, J., and G.M. Pound, J. Chem. Phys., Vol.22, 1942, p.1.
16. Harding, L. J., "A Digital Computer Program for Condensation in Expanding One-Component Flows," (Univ. of Mich.) USAF Aerospace Research Labs., OAF, ARL 65-58, March 1965.
17. Wegener, P.P., and L.M. Mack, "Condensation in Supersonic and Hypersonic Wind Tunnels," Adv. in Appl. Mech., Vol.V, Academic Press, 1958, pp.307-447.
18. Courtney, W.G., "Homogeneous Nucleation from Simple and Complex Systems," AIAA Preprint No.63-494, presented at the AIAA Heterogeneous Combustion Conference, 11-13 December 1963.
19. Wegener, P.P., and A.A. Pouring, "Experiments on Condensation of Water Vapor by Homogeneous Nucleation in Nozzles," Physics of Fluids, Vol.7, No. 33, pp.352-361, March 1964.
20. Lothe, J., and G.M. Pound, "Reconsiderations of Nucleation Theory," J. Chem. Phys., Vol.36, No.8, 15 April 1962, pp.2080-2085.
21. Courtney, W.G., "Re-examination of Nucleation and Condensation of Water," Technical Report, Thiokol Chemical Corp., Reaction Motors Division, Denville, N.J., July 1964.
22. Tables of Thermal Properties of Gases, NBS Circular 564, U.S. Government Printing Office, Washington, D.C., 1955.
23. Vas, I. E., and G. Koppenwallner, "The Princeton University High Pressure Hypersonic Nitrogen Tunnel N-3," (Princeton U. Gas Dynamics Lab., Rpt.690), United States Air Force, Office of Scientific Research Report AFOSR 64-1422, July 1964.
24. Griffith, B. J., H. E. Deskins, and H. R. Little, "Condensation in Hotshot Tunnels," Arnold Engineering Development Center Report AEDC-TDR-64-35, February 1964.
25. Daum, F.L., "The Condensation of Air in a Hypersonic Wind Tunnel," IAS Paper No.63-53, presented at the IAS 31st Annual Meeting, 21-23, January 1963. (Also published in the AIAA J., Vol.1, No.5, May 1963, pp.1043-1046).
26. Reiss, H., "Theory of the Liquid Drop Model," Ind. Eng. Chem., Vol.44, 1952, p.1284.
27. Jaeger, H. L., "Condensation of Supersaturated Ammonia and Water Vapor in Supersonic Nozzles," Gas Turbine Laboratory Report No.86, M.I.T., 1966.

Appendix A

USER'S MANUAL – ONE-DIMENSIONAL FLOW/
MULTI-SPECIE CONDENSATION PROGRAM

Appendix A

A.1 INTRODUCTION

This user's manual describes a digital computer program designed to predict multiple-specie condensation phenomena in a one-dimensional flow. The program is written in FORTRAN IV language and has been checked out on the Univac 1108, IBM 7094 and EAI 8400 computer systems. The theory of the problem is described in Appendix B; this appendix describes the present capabilities of the program and gives an input guide to aid the engineer in using the program. This program solves the condensation problem of a 1-D jet expansion into a vacuum for several species. The multiple-specie system takes advantage of homogeneous nucleation and allows for heterogeneous droplet growth. The condensation phenomenon is related to the flow through the mass fraction of condensate, which causes the available volume of the gaseous state to reduce as the amount of condensate increases. Isentropic flow equations are used to describe the system until the onset of condensation occurs. The flow equations linked with condensation are then used to describe the remaining flow field. The vapor phase is assumed to be a pure vapor and is treated as a perfect gas. Dalton's law of partial pressures is used to derive specie pressures from the flow pressure.

Solutions to the problem are obtained by a convergence of total mass fraction of condensate within the flow equations. The condensation-linked flow equations are solved by using a Euler's method of solution. This method is dependent upon a small nozzle increment in the longitudinal direction for an exact numerical solution to the nonlinear differential equations. Initial values of parameters are assumed and iterated upon until convergence is obtained.

This appendix discusses the capabilities of the One-Dimensional Flow/Multiple Species Condensation program including a description of subroutines. An input guide and output description is given as an aid to the user.

A.2 PROGRAM CAPABILITIES AND SUBROUTINE DESCRIPTION

A.2.1 General

The computer program discussed herein determines the influence of the condensation process in effecting expansion of vapors and heat transfer. The program was designed to handle multiple species assuming chemical equilibrium between species and phases. The condensation equations, which are the homogeneous nucleation rate equation, heterogeneous droplet growth equation and specie mass fraction equation are linked to the nonlinear differential flow equations through a mass fraction dependency of gaseous and mixture densities, a variable gaseous mixture molecular weight and the net energy exchange between condensate and flow. A diagram of the basic program logic is given in Fig. A-1. The diagram basically shows that before condensation can occur, $NCS \neq 0$ (number of condensable species is not equal to zero, or, the isentrope must have crossed a specie vapor pressure curve), and the r^* criteria must be passed (droplets must nucleate to the critical size of equal probability of condensation and evaporation). The final solution gives the condensation effects upon both thermodynamic and flow properties.

A.2.2 Program Capabilities

The One-Dimensional Flow Multi-Specie Condensation Program is a useful tool for the thermodynamics, aerodynamics and chemical engineer for flowfield studies in plume impingement and contamination problems. It provides a detailed one-dimensional flowfield analysis and easily predicts which specie will condense, if any, and how much condensation will occur. A summarized list of the present program capabilities is shown on page A-4.

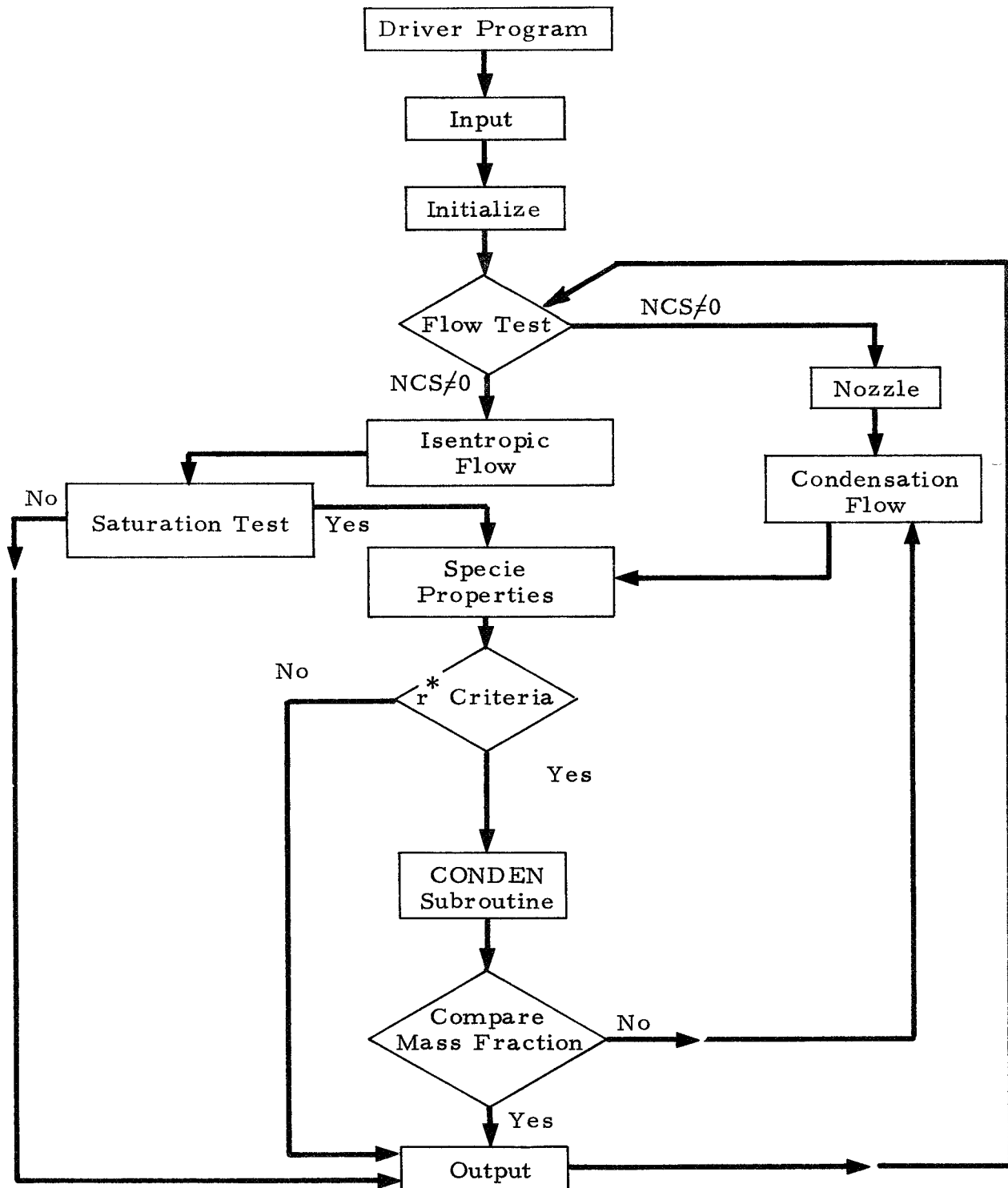


Fig. A-1 - Flow Chart of Condensation in Expanding Flow Program

- Homogeneous or pure vapor expansion analysis
- One condensable specie analysis in a carrier gas
- Multiple condensing species analysis
- Isentropic expansion without condensation
- Energy transfer between condensate and flow
- Droplet temperature analysis
- One-dimensional plume analysis
- Prediction of mass fraction of condensate

A.2.3 Subroutine Description

This section explains the subroutines used in the digital program. Communication between the subroutines is via COMMON blocks. The program consists of a driver and 16 subroutines. The summarized logic and functions of the subroutines are as follows:

- MAIN

This is the driver program with the logic either for isentropic flow or for flow with condensation; testing for the crossing point of the expansion isentrope with a specie vapor pressure curve; calculating the critical radius and testing for the size criteria; and testing for mass fraction convergence of the flow solution. Subroutines called by MAIN are: INPUT, INIT, IFLOW, NOZZLE, CFLOW, SPROP, CONDEN, OUTPUT and ERROR.

- INPUT

This subroutine is designed to read and print all input data for the One-Dimensional Flow/Multi-Specie Condensation Program. Another function of INPUT is to calculate the specie mole fractions from the input data.

- BLOCK

This is a BLOCK DATA subprogram, compiled with the deck, and not called from any subroutine. It consists of constants, convergence criteria and loop limits.

- INIT

This subroutine initializes all necessary variables for each case to be run. Each specie saturation point is calculated on the mixture isentrope. INIT also calculates nozzle throat conditions.

- IFLOW

IFLOW is programed to evaluate the one-dimensional isentropic flow equations. It also calls subroutines CPOFT, NOZZLE and PITOT.

- CPOFT

This subroutine calculates specie and mixture specific heat at constant pressure as a function of temperature.

- NOZZLE

If NOZZLE(1) is called, nozzle position is calculated as a function of nozzle cross-sectional area. If NOZZLE(2) is called, nozzle cross-sectional area is calculated as a function of nozzle position. This subroutine handles wedges, cones or any nozzle profile read in by subroutine INPUT.

- PITOT

This subroutine is intended to calculate pitot pressure as a function of nozzle position. It is at present only a dummy subroutine and is not used. The user can supply one if desired.

- CFLOW

CFLOW evaluates the condensation linked flow equations. It calls subroutines CPOFT, LATOFT, QOFT and PITOT.

- LATOFT

This subroutine calculates latent heat as a function of temperature.

- QOFT

QOFT computes the energy exchange between gas and condensate accounting for the phase change and temperature differences between flow and condensed droplets; i.e., heat transfer.

- SPROP

SPROP computes liquid density, surface tension and saturation vapor pressure as a function of flow temperature for each condensable specie.

- EXPF

This subroutine limits the exponential computations so that computer limitations are bypassed to avoid possible numerical overflow. EXPF is called by CONDEN, SPROP and DPROP.

- CONDEN

CONDEN is the primary routine for multi-specie condensation analysis in expanding flows. The subroutine calculates specie nucleation rate, droplet growth rate, droplet temperature and pressure, radii of drops, number of drops, mass growth of drops and mass fraction of condensate and recomputes specie mole-fraction, molecular weight and mixture gas constant.

- DPROP

This subroutine calculates liquid density, surface tension, vapor pressure and other properties as a function of droplet temperature for both homogeneous and heterogeneous liquids.

- OUTPUT

OUTPUT prints the results of the program execution. It also saves values one nozzle length upstream which are necessary for the Euler method of solution of flow equations.

- ERROR

This subroutine is designed to print out messages if iteration loop limits are reached due to divergence of the numerical methods.

A.3 INPUT GUIDE

This section serves as the guide for the engineer to prepare data for the One-Dimensional Flow/Multi-Specie Condensation Program. All inputs to the program are read from cards supplied by the user; no additional tapes are required. Basic inputs include a title card, case control card, specie mass fraction card, specie molecular weight card, nozzle description card, thermodynamic condition card, mass accommodation coefficients, units of pressure, coefficients for saturation pressure, coefficients for liquid density, coefficients for specific heat and surface tension. The run is terminated by an ENDM card, starting in column 1, at the end of the data. If the card is not there, a new data case will be expected or an abnormal termination will occur.

A.3.1 Input Card Description

All properties must be input in a decreasing order as the specie becomes a potential condensable.

<u>Card</u>	<u>Variable</u>	<u>Format</u>
1	TITLE	20A4
2	NS, NTRUN, NCR, NCL, NCCP, NCSIG, IDEBUG	14I5
3	FRAMAS(I)	6E10.0
4	AW(I)	6E10.0
5*	IGEOM, XINIT, XEND, THETAC, THETAD, ASTAR, DELX, INOZ	A4, IX, 6E10.0, I5
6	TZ, PZ, DELTZ, DELTIS, RCRIT, PGUESS	6E10.0
7	XA(I)	6E10.0
8	PUNIT(I)	6E10.0
9**	ASAT(I), BSAT(I)	6E10.0
10***	CR(I, J)	6E10.0
11***	CL(I, J)	6E10.0
12***	CCP(I, J)	6E10.0
13***	CS(I, J)	6E10.0
14	TOLMAN(I)	6E10.0
15	ENDM	A4

The description of the program variables is presented on page A-9.

* More nozzle description cards may exist here depending upon INOZ. This is explained in the input variable descriptions.

** Up to three species are input on one card. Two cards for four and up to five species if necessary.

*** J number of coefficients for each specie I. Each specie requires a separate card.

<u>Variable</u>	<u>Description</u>
TITLE	Title for problem identification.
NS	Total number of species in the system.
NTRUN	Total number of stagnation temperatures to be run for each case.
NCR	Number of temperature-dependent coefficients for <u>density</u> .
NCL	Number of temperature-dependent coefficients for <u>latent heat</u> .
NCCP	Number of temperature-dependent coefficients for <u>specific heat at constant pressure</u> .
NCSIG	Number of temperature-dependent coefficients for <u>surface tension</u> .
IDEBUG	Intermediate printout control. IDEBUG = 0 No printout ≠ 0 Intermediate printout
FRAMAS(I)	The initial specie i mass fraction.
AW(I)	The molecular weight of specie i.
IGEOM	Parameter used to identify cross-sectional geometry of nozzle. IGEOM = WEDGE, rectangular geometry = CONE, circular geometry
XINIT	The initial nozzle position (upstream of throat, cm)
XEND	The longitudinal position along the nozzle centerline at which the last calculation will take place (cm).
THETAC	The half angle in degrees of the converging portion of the nozzle.
THETAD	The half angle in degrees of the diverging portion of the nozzle.
ASTAR	Throat area of nozzle (cm ²).
DELX	The longitudinal integration step along the nozzle centerline (cm).
INOZ	An option for the nozzle profile input. INOZ = 0, no profile input necessary, the nozzle is assumed to be either a cone or a wedge.(depending on IGEOM). INOZ = -1, this option allows a nozzle profile to be input in the form of discrete points. It will calculate rectangular cross-sectional areas (nozzle radius versus X).

<u>Variable</u>	<u>Description</u>
INOZ	INOZ = 1, this option is similar to the option INOZ = -1 except it will calculate circular cross-sectional areas (nozzle radius vs X). INOZ = 2, this option allows any geometrically shaped <u>area</u> versus <u>nozzle</u> position input.

If INOZ reads anything other than 0 then the following input cards are expected:

NPTS	The number of points to be read in from the nozzle profile, FORMAT(I5).
XTAB(I), ATAB(I)	The nozzle distance input in centimeters, the area or vertical distance to the nozzle profile (centimeter units). They must be input as a set and increasing along the nozzle position. FORMAT(6E10.0).
TZ	Chamber temperature ($^{\circ}\text{K}$).
PZ	Chamber pressure (dynes/cm^2).
DELTZ	A variable which will reduce the chamber temperature by the value DELTZ to obtain additional computer runs ($^{\circ}\text{K}$).
DELTIS	The temperature increment at which the isentropic flow routine will calculate the flow variables ($^{\circ}\text{K}$).
RCRIT	The radius of the nuclei at which time the nucleation equations commence (cm).
PGUESS	An initial guess of the pressure at which the expansion process crosses the first condensable specie vapor pressure curve (dynes/cm^2).
XA(I)	The mass accommodation coefficient for each specie.
PUNIT(I)	The pressure units at which the vapor pressure coefficients are derived.

$$1.0 \frac{\text{dynes/cm}^2}{\text{dynes/cm}^2} \quad \text{or,}$$

$$1.013 \times 10^6 \frac{\text{dynes/cm}^2}{\text{atm}}$$

<u>Variable</u>	<u>Description</u>
ASAT(I)	The first vapor pressure coefficient of specie I.
BSAT(I)	The second coefficient of the vapor pressure curve of specie I.
CR(I, J)*	The polynomial coefficients describing the density of specie I.
CL(I, J)*	The polynomial coefficients describing the latent heat of specie I.
CCP(I, J)*	The polynomial coefficients describing the C_p/R ratio of specie I.
CS(I, J)*	The polynomial coefficients describing the flat plate equilibrium surface tension of specie I.
TOLMAN(I)	The Tolman constant, or surface tension correction term, (cm).
ENDM	A variable which when read will cease program operation. It represents an option of the title card to cease or continue data cases.

A sample input form is shown in Fig. A-2 to aid the user in inputting the program.

*The polynomial curve fits are in the following form:

$$\rho_i = \sum_{j=1}^{NR} C R_{ij} T^{j-1}$$

```

AIR-1.5-PER CENT WATER VAPOR TO COMPARE WITH MIT EXPERIMENTAL DATA
      2      1      2      2      2      2      0      0
      .015      .985
      18.016      28.967
CONE -3.810      30.0      1.      1.      .31669      .05      00001
      29
-3.810      0.3400      -2.540      0.3330      -1.270      0.3230
      0.0      0.3175      1.270      0.3230      2.540      0.3330
      3.810      0.3400      5.080      0.3510      6.350      0.3580
      7.620      0.3680      8.890      0.3750      10.160      0.3840
      11.430      0.3910      12.700      0.3990      13.970      0.4090
      15.240      0.4140      16.510      0.4220      17.780      0.4320
      19.050      0.4390      20.320      0.4470      21.590      0.4550
      22.860      0.4620      24.130      0.4670      25.400      0.4750
      26.670      0.4830      27.940      0.4880      29.210      0.4950
      30.480      0.5030      31.623      0.5080
      381.07      8.37500E06      0.0      2.0      1.000E-07 40000.0
      .04      0.0
      1.      1.
      27.9671      5259.0      25.7      882.0
      .9      0.0
      1.177      .00476
      3.2333E10      -2.7125E7
      2.3000E09      0.0
      4.006      0.0
      3.440      0.0
      122.33      -.1692
      25.8      -.22
      .475E-8      0.0
ENDM

```

Fig. A-2 - Sample Data Input

A.4 OUTPUT GUIDE

This section serves as a guide for the user to recognize output notation of the One-Dimensional Flow/Multi-Specie Condensation program. The description and engineering units are included for each output parameter.

<u>Parameter</u>	<u>Description and Units</u>
X	nozzle distance from the throat (cm)
P	mixture static pressure (dynes/cm ²)
T	mixture static temperature (°Kelvin)
RHO	mixture density (gm/cm ³)
V	velocity (cm/sec)
M	Mach number (dimensionless)
GAMMA	ratio of specific heats (dimensionless)
A	cross-sectional nozzle area (cm ²)
RVA	mass flow rate (gm/sec)
MU	mass fraction of condensate (dimensionless)
NJ	specie nucleation rate (drops/sec-cm ³)
TMASS	specie total condensed mass (gm)
RSTAR	specie critical radius (cm)
RAD L	radius of largest (1st) drop (cm)
DROPS	droplet number density (drops/cm ³)
TDL	temperature of the largest drop (°Kelvin)
TDS	temperature of the smallest drop (°Kelvin)
NCS	number of condensable species (as description)
KTYPE	number of droplet types (as description)

When the output parameter involves specie identification, such as NJ, TMASS and RSTAR, the printout value is listed in the same descending order of potential condensable as the input requirement.

Appendix B

DEVELOPMENT OF NUCLEATION RATE AND DROP
GROWTH EQUATIONS FOR MULTIPLE SPECIES

Appendix B

B.1 DEVELOPMENT OF THE HOMOGENEOUS NUCLEATION RATE EQUATION

Most nucleation rate theory is based in an essentially chemical terminology. The following derivation is in keeping with this terminology and follows the classical nucleation theory of Frenkel (Ref. B.1). This derivation is intended to point out assumptions made in the classical derivations and to include the terms that account for multi-component effects.

Phase transitions are dependent on the availability of surfaces of condensation, which may be walls of a vessel or condensed nuclei contained in the vapor. Phase transition based on nuclei of different species is termed condensation by "heterogeneous nucleation." In the absence of foreign nuclei, the appearance of liquid in a vapor is dependent on small clusters formed by fluctuations in the parent phase and is termed "homogeneous nucleation." The classical nucleation theory neglects intermolecular forces and states that from kinetic theory the distribution of clusters of vapor molecules is described by a Boltzmann distribution. The resulting expression of nucleation rate (i.e., number of nuclei formed per unit time and volume) is given by

$$N(g) = N_o e^{(-\Delta G/kT)} \quad (B.1)$$

where

- N_o = total number of molecules
- G = $H - TS$ (Gibbs free energy)
- ΔG = the change in Gibbs free energy in forming a cluster of g molecules.

The main problem in adequately modeling the nucleation process is in determining a realistic expression of the change in Gibbs free energy, ΔG . The term is usually described by assigning macroscopic thermodynamic

properties to critical nuclei. This practice is permissible for large nuclei, but is questionable for clusters consisting of less than 20 molecules (Ref. B.2).

Classically, the change in Gibbs free energy consisted of two parts: (1) the reversible work effect of condensation to the bulk phase, ΔG_b , and (2) the work required to produce a free surface, ΔG_a . Lothe and Pound (Ref. B.3) showed that there are three additional terms to the change in free energy, the first of which is the free energies of separation given by

$$\Delta G_s \cong kT \ln(2\pi g)/2 + 5kT \quad (B.2)$$

which is due to the separation per droplet of g molecules plus a term required for conservation of degrees of freedom of molecules.

The second term is a contribution to the free energy from the translational degrees of freedom of the cluster. The translational free energy is given in terms of the partition function as

$$\Delta G_{E_t} = -kT \ln \left[(2\pi m kT)^{3/2} \Omega / h^3 \right] \quad (B.3)$$

where

m = molecular mass of the clusters

Ω = cluster molecular volume in the gaseous standard state at P and T

The third additional contribution is a rotational contribution to the entropy and free energy arising from energizing the droplets to form a gas of the clusters. Assuming a spherical droplet, the rotational free energy of formation of a cluster is

$$\Delta G_{E_r} = -kT \ln \left[(2kT)^{3/2} (\pi I^3)^{1/2} / h^3 \right] \quad (B.4)$$

Therefore, according to Lothe and Pound (Ref. B.3) the net Gibbs free energy change of formation of a critical cluster in homogeneous nucleation of droplets from a vapor is

$$\Delta G = \Delta G_b + \Delta G_a + \Delta G_s + \Delta G_{E_t} + \Delta G_{E_r} \quad (B.5)$$

Results of the classical derivation have given good results; therefore the last three terms of Eq. (B.5) are neglected for this approach. The work of Lothe and Pound (Ref. B.3) is briefly stated as a reminder of the complexity of the nucleation theory.

Consider the approximations made in obtaining the classical form of the change in Gibbs free energy for bulk phase transition. The general expression for Gibbs free energy of a thermally perfect gas mixture is

$$G_b = \sum_i^n \mathcal{N}_i \left[\bar{\mu}_i(T) + R T \left(\ln P + \ln \frac{N_i}{N} \right) \right] \quad (B.6)$$

where

i represents the subscript of a specie and,

$$\bar{\mu}_i = \int_{T_o}^T C_{P_i} dT - T \int_{T_o}^T C_{P_i} \frac{dT}{T} + h_{o_i} - T S_{o_i} - R T \ln P_o$$

The term $\bar{\mu}_i$ is the specie chemical potential and is a function of temperature only. A phase transition is considered to be a constant temperature process. Therefore, in computing ΔG_b the chemical potential term cancels, resulting in the following expression

$$\Delta G_{b_i} = \sum_i^n \left(G_{b_2} - G_{b_1} \right)_i = \sum_i^n \mathcal{N}_i R T (\ln P_{2i}/P_o) - \sum_i^n \mathcal{N}_i R T (\ln P_{1i}/P_o)$$

or

$$\Delta G_{b_i} = - \sum_i^n \mathcal{N}_i R T \ln(P_{1i}/P_{2i}) = - \sum_i^n g_i k T \ln(P_i/P_{\infty_i}) \quad (B.7)$$

The P_∞ is equal to the flat surface equilibrium pressure of a formed embryo of g molecules and P is the existing local pressure. Note that for one specie Eq. (B.7) reduces to the classical expression $\Delta G_b = -gkT \ln(P/P_\infty)$.

In keeping with the classical model spherical drop assumption,

$$\Delta G_{a_i} = 4\pi r_i^2 \sigma_i \quad (B.8)$$

The uncertainties associated with the physical phenomena occurring in condensation restrict this derivation to the first two terms of Eq. (B.5). This assumes that the spherical drop is stationary in the vapor system and has no rotational or vibrational energy. The droplet is also assumed to form at environmental temperature. Therefore $N(g)$ can be written:

$$N(g) = \left[\sum_{i=K}^n N_{o_i} \right] e^{-\left(\sum_i^n g_i \ln(P_i/P_{\infty_i}) - \sum_i^n \Delta G_{a_i}/kT \right)} \quad (B.9)$$

A criterion for condensation is if $P_i < P_{\infty_i}$, then $K = i$, where K is the number of condensable species.

For a single specie, Eq. (B.9) reduces to the classical derivation expression for the number of nuclei formed per unit time and volume. For two species, however, three nucleation possibilities exist (i.e., I, II and I + II). Heterogeneous nucleation requires further investigation and is not included in this analysis. Assuming that there is homogeneous nucleation only of all species, Eq. (B.9) becomes

$$N_i(g) = N_{o_i} e^{\left(g_i \ln(P_i/P_{\infty_i}) - 4\pi r_i^2 \sigma_i/kT \right)} \quad (B.10)$$

$N_i(g)$ is therefore the Boltzmann distribution or the distribution of clusters of vapor molecules resulting from the kinetic interaction of similar molecules of K condensable species. Following the analysis of Frenkel (Ref. B.1)

$$g_i m_i = \frac{4}{3} \pi r_i^3 \rho_{L_i} . \quad (B.11)$$

Substitution of r_i into Eq.(B.10) yields

$$N_i(g) = N_{o_i} e^{\left\{ g_i \ln \left(\frac{P_i}{P_{\infty_i}} \right) - \frac{4 \pi \sigma_i}{kT} \left(\frac{3 g_i m_i}{4 \pi \rho_{L_i}} \right)^{2/3} \right\}} \quad (B.12)$$

and saying that

$$\epsilon_i = 4 \pi \sigma_i \left(\frac{3 m_i}{4 \pi \rho_{L_i}} \right)^{2/3} ,$$

Eq. (B.12) reduces to

$$N_i(g) = N_{o_i} e^{\left\{ g_i \ln \left(\frac{P_i}{P_{\infty_i}} \right) - \frac{\epsilon_i}{kT} g_i^{2/3} \right\}} \quad (B.13)$$

The system in the classical derivation is treated as one in a state of quasi-equilibrium in which the droplets are imagined to condense after reaching a size larger than the critical radius r_i^* that occurs at the maximum of the supersaturated free energy change.

The maximum of free energy change (minimum in $N_i(g)$) occurs when

$$\frac{d}{dg} (\Delta G_i) = 0 = -kT \ln \left(\frac{P_i}{P_{\infty_i}} \right) + \frac{2}{3} \epsilon_i g_i^{-1/3}$$

Therefore,

$$kT \ln\left(\frac{P_i}{P_{\infty_i}}\right) = \frac{2}{3} \epsilon_i g_i^{-1/3}$$

From Eq. (B.13), the Gibbs free energy term is

$$\Delta G_i = -g_i kT \ln\left(\frac{P_i}{P_{\infty_i}}\right) + \epsilon_i g_i^{2/3}$$

and

$$\Delta G_{i_{\max}} = -\frac{2}{3} \epsilon_i g_i^{2/3} + \epsilon_i g_i^{2/3} = \frac{1}{3} \epsilon_i g_i^{2/3} = \frac{4\pi}{3} r_i^{*2} \sigma_i$$

Then

$$\Delta G_{i_{\max}} = -g_i kT \ln\left(\frac{P_i}{P_{\infty_i}}\right) + 4\pi r_i^{*2} \sigma_i = \frac{4\pi}{3} r_i^{*2} \sigma_i \quad (B.14)$$

Solving Eq.(B.14) for $\ln\left(\frac{P_i}{P_{\infty_i}}\right)$ yields

$$\ln\left(\frac{P_i}{P_{\infty_i}}\right) = \frac{2 m_i \sigma_i}{\rho_{L_i} k T r_i^* N_A} \quad (B.15)$$

Equation (B.15) called the Kelvin-Helmholtz expression, describes the equilibrium conditions of a liquid drop with its vapor phase.

In assuming a quasi-equilibrium state and ignoring the interaction between nuclei, the nucleation rate must be independent of g so that the number of droplets of any size remains constant and the rate at which droplets of larger size are removed from the system is equal to the nucleation rate. In the same manner, single molecules are added to the system at a rate equal to the depletion due to nucleation.

By assuming that the growth of nuclei occurs only from the interaction with free molecules, the interaction rate is

$$J_i(g+1, t) = \beta_i S_i(g) \times \eta_i(g, t) - \gamma_i(g+1) S_i(g+1) \eta_i(g+1, t) \quad (B.16)$$

where

β_i = rate at which molecules strike unit surface area of specie i.

$\gamma_i(g)$ = rate at which molecules leave unit surface area of specie i.

$\eta_i(g, t)$ = distribution of non-equilibrium drops of specie i.

$S_i(g)$ = surface area of g_i sized drops.

Assuming that there is no cluster motion and there are no droplet curvature effects, kinetic theory yields

$$\beta_i = \frac{P_i}{(2\pi m_i kT)^{1/2}}$$

If the nucleation rate is zero, then the quasi-equilibrium distribution $\eta_i(g)$ is equal to the equilibrium distribution $N_i(g)$. The mathematical statements are,

$$\text{when } J_i(g, t) = 0$$

$$\beta_i S_i(g) \eta_i(g) = \gamma_i(g+1) S_i(g+1) \eta_i(g+1)$$

$$\text{then } \eta_i(g) = N_i(g)$$

Therefore,

$$\beta_i S_i(g) N_i(g) = \gamma_i(g+1) S_i(g+1) N_i(g+1).$$

Equation (B.16) then becomes

$$J_i(g, t) = \beta_i S_i(g) N_i(g) \left[\frac{\eta_i(g, t)}{N_i(g)} - \frac{\eta_i(g+1, t)}{N_i(g+1)} \right] \quad (B.17)$$

Assuming a large number of molecules in a droplet cluster, the functions can be treated as continuous. Equation (B.17) therefore becomes approximately:

$$J_i(g, t) = \beta_i S_i(g) N_i(g) \frac{d}{dg} \left(\frac{\eta_i}{N_i} \right)$$

and since

$$J_i(g, t) = J_i(t) ,$$

$$\int d \left(\frac{\eta_i}{N_i} \right) = \frac{J_i}{\beta_i} \int \frac{dg}{S_i(g) N_i(g)} \quad (B.18)$$

Using two boundary conditions from Fig. B-1 , (Duff (Ref. B.4)),

$$(a) \frac{\eta_i}{N_i} = 1.0 \text{ at } g_i = 1 \quad (b) \lim_{g_i \rightarrow \infty} \frac{\eta_i}{N_i} = 0$$

Equation (B.18) becomes

$$J_i = \frac{\beta_i}{\int_1^\infty \frac{dg}{S_i N_i}} \quad (B.19)$$

At the vicinity of $g_i = g_i^*$, the expression $\frac{1}{N_i} = \frac{1}{N_{o_i}} e^{\left(\frac{\Delta G_i}{kT} \right)}$ has a sharp

maximum. Therefore, Eq. (B.19) may be approximated by:

$$J_i = \frac{\beta_i S_i(g_i^*) N_{o_i}}{\int_1^\infty e^{\left(\frac{\Delta G_i}{kT} \right)} dg} \quad (B.20)$$

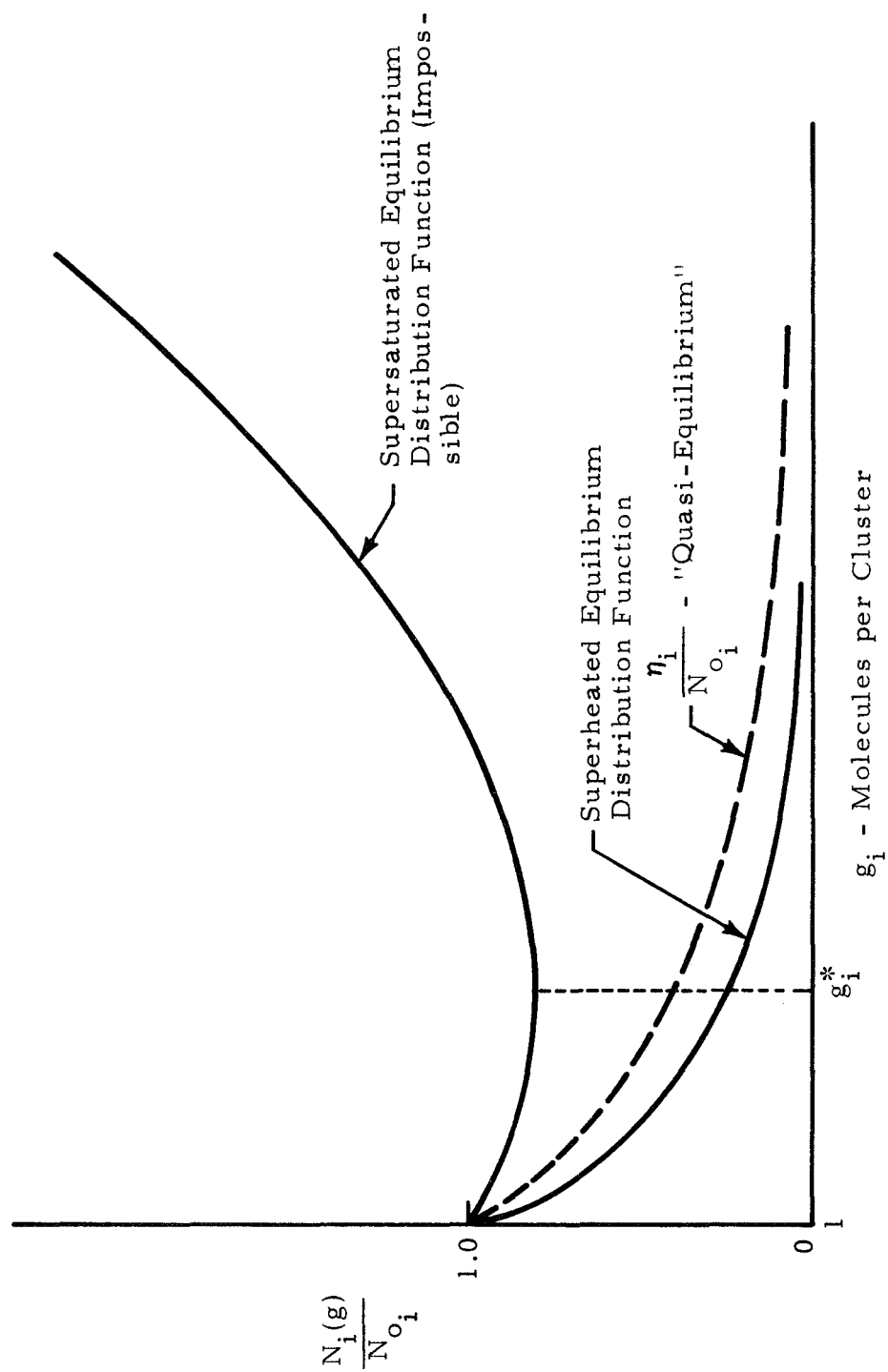


Fig. B-1 - General Form of Cluster Size Density Distributions for One Species i

Incorporation of Eqs. (B.11), (B.12) and (B.15) yields

$$\frac{\Delta G_i}{kT} = -g_i \ln \frac{P_i}{P_{\infty_i}} + \frac{\epsilon_i}{kT} g_i^{2/3}$$

$$\frac{\Delta G_i}{kT} = -g_i \left[\frac{2 m_i \sigma_i}{\rho_{L_i} kT r_i^*} \right] + \frac{4 \pi \sigma_i}{kT} \left[\frac{3 m_i}{4 \pi \rho_{L_i}} \right]^{2/3} g_i^{2/3}$$

and

$$\frac{\Delta G_i}{kT} = A_i \left[3 \left(\frac{g}{g^*} \right)_i^{2/3} - 2 \left(\frac{g}{g^*} \right)_i \right]$$

where

$$A_i = \frac{\sigma_i m_i}{\rho_{L_i} kT} \left(\frac{4 \pi \rho_{L_i}}{3 m_i} \right)^{1/3} g_i^{*2/3} = \frac{4 \pi \sigma_i r_i^{*2}}{3 kT}$$

Therefore Eq. (B.20) may be written as

$$J_i = \frac{\beta_i S_i(g^*) N_{O_i}}{\int_1^\infty e^{\left\{ A_i \left[3 \left(\frac{g}{g^*} \right)_i^{2/3} - 2 \left(\frac{g}{g^*} \right)_i \right] \right\}} dg} \quad (B.21)$$

Equation (B.21) is solved approximately by the introduction of

$$\Omega_i = \left(\frac{g}{g^*} \right)_i^{1/3} - 1 \quad (B.22)$$

The limits of the integral in Eq. (B.21) may be taken at $+\infty$ and $-\infty$ since the integrand of Eq.(B.21) has a sharp maximum e^{A_i} at $g_i = g_i^*$ and the important values of Ω_i are small.

Because

$$\left(\frac{g}{g_i^*}\right)^{2/3} = \Omega_i^2 + 2\Omega_i + 1$$

$$dg = 3(1 + \Omega)^2 g_i^* d\Omega$$

and

$$3\left(\frac{g}{g_i^*}\right)^{2/3} - 2\left(\frac{g}{g_i^*}\right) = -3\Omega_i^2 - 2\Omega_i + 1$$

The integral portion of Eq. (B.21) upon substitution of the above equations may be written as

$$\begin{aligned} 3 g_i^* e^{A_i} \int_{-\infty}^{+\infty} (1 + \Omega_i)^2 e^{(-3 A_i \Omega_i^2 - 2 A_i \Omega_i^3)} d\Omega &\simeq 3 g_i^* e^{A_i} \int_{-\infty}^{+\infty} e^{(-3 A_i \Omega_i^2)} d\Omega \\ &= 3 g_i^* e^{A_i} \left(\frac{\pi}{3 A_i}\right)^{1/2} \end{aligned} \quad (B.23)$$

Substitution of Eq. (B.23) into Eq. (B.21) yields

$$J_i = \frac{\beta_i S_i (g_i^*) N_{o_i} \left[\frac{A_i}{3\pi}\right]^{1/2}}{g_i^*} e^{-A_i} \quad (B.24)$$

where

$$N_{o_i} = \frac{P_i}{kT}$$

$$\beta_i = \frac{P_i}{(2\pi m_i kT)^{1/2}}$$

$$S_i(g^*) = \frac{\epsilon_i (g_i^*)^{2/3}}{\sigma_i}$$

Inserting the expressions for ϵ_i and A_i , Eq. (B.24) may be written as

$$J_i = \left(\frac{P_i}{kT}\right)^2 \frac{m_i}{\rho_{L_i}} \left(\frac{2\sigma_i}{\pi m_i}\right)^{1/2} e^{\left(\frac{-4\pi\sigma_i r_i^{*2}}{3kT}\right)} \quad (\text{B.25})$$

The expression defines the number of nuclei of specie i formed per unit volume per unit time. It is identical to the expression of the classical derivation. For the multi-component case, therefore, the nucleation equation must be applied to each condensable specie.

B.2 DEVELOPMENT OF HETEROGENEOUS DROPLET GROWTH AND SPECIE MASS ANALYSIS

The mechanism of heterogeneous droplet growth onto droplets formed by homogeneous nucleation requires a concise mathematical model to describe growth discontinuities of the droplets. Assume that the homogeneous nucleation rate equations hold and that the molecular velocity distributions are Maxwellian before and after collision and accommodation with droplet surface.

For illustration purposes, assume three condensable species in a mixture of gas. The mechanism of heterogeneous droplet growth is assumed to occur as shown in the schematic of Fig. B-2. The heterogeneous droplets are designated as growth onto homogeneous nuclei of species 1, 2 and 3. Discontinuities, due to mass addition of different specie molecules in the form of condensates, are designated by Roman numerals. Specifically, I indicates the position in the nozzle where the critical radius of the first condensable specie has been reached. The quasistatic volume where I occurs is designated as $A(X_1) \Delta X_1$. It is assumed that critical sized droplets of specie 1 occur in all ΔX regions. Homogeneous droplet growth equations hold until the discontinuity II. At this axial position, the vapor pressure of the second condensable specie reaches its saturation pressure. Heterogeneous growth of two species commences at II and terminates at IV, where heterogeneous growth of three species commences. The discontinuity at III is the position in the nozzle where the critical radius of the second condensable specie has been reached. Homogeneous nucleation of specie 2 to the critical droplet size is assumed to occur in all ΔX regions following III. The region from IV to V shows growth of three species onto heterogeneous droplets formed by specie nucleates 1 and 2. The critical droplet size of specie 3 just occurs at position V and is assumed to occur in all ΔX regions that follow. Growth of all specie molecules onto droplets formed by all three

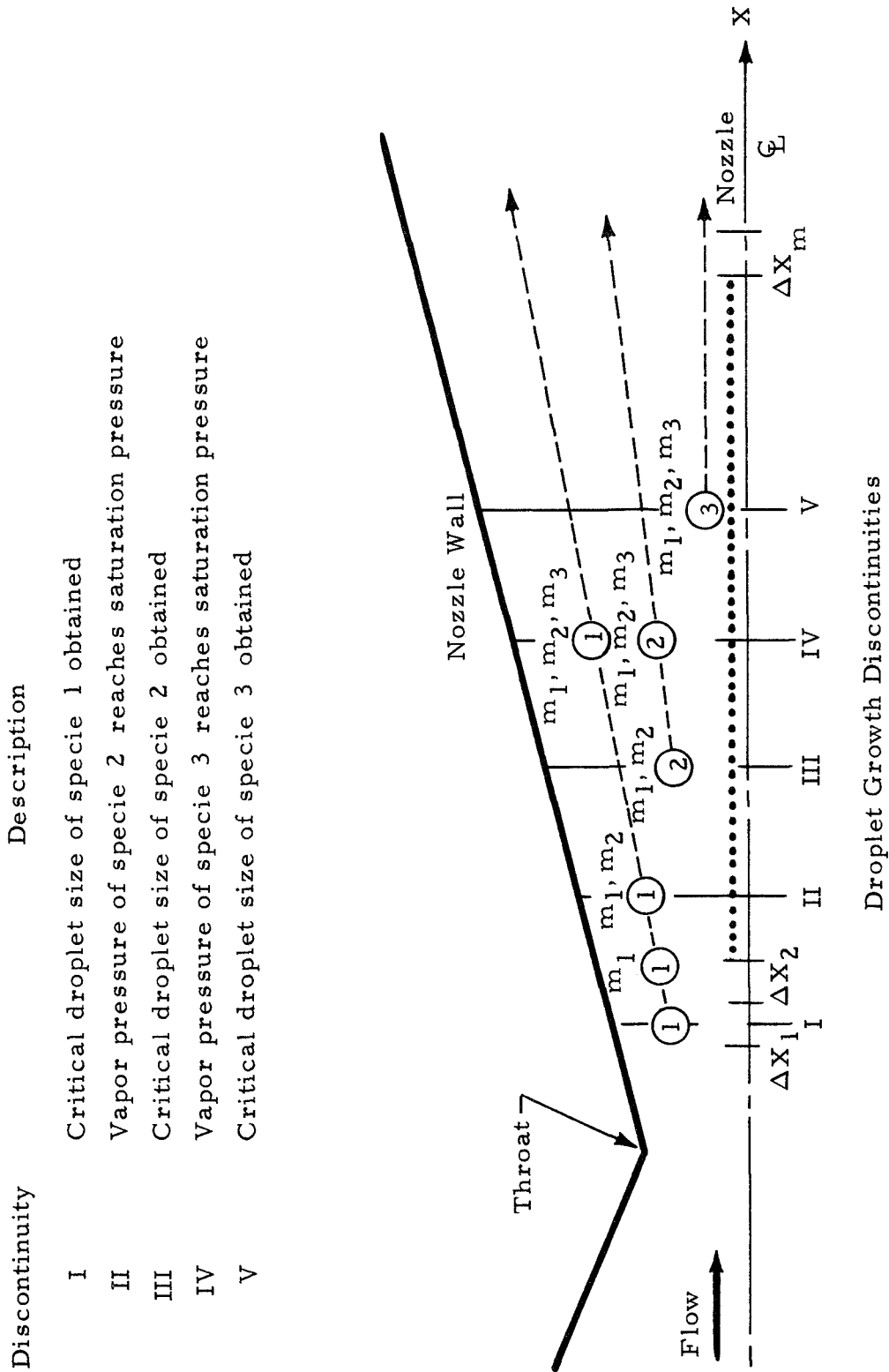


Fig. B-2 - Schematic of Three Specie Heterogeneous Droplet Growth

specie nucleates occurs after region V. The mechanism for additional condensable species would follow the same criteria.

Newly formed droplets in each ΔX must grow according to the growth described within each discontinuity range (i.e., Range I-II yields growth of specie 1; Range II-IV yields growth of species 1 and 2; and position IV marks the beginning of growth of species 1, 2 and 3). The heterogeneous droplet growth equation is derived using the nomenclature of Section B.1. Let the subscript j be a droplet of any composition. The total condensed mass rate per unit area onto a droplet j of k condensed species is

$$\sum_i^K \frac{\xi_i P_i}{(2\pi R_i T)^{1/2}}$$

The mass rate per unit area which has evaporated is

$$\sum_i^K \frac{\xi_i P_{D_j}}{(2\pi R_i T_{D_j})^{1/2}}$$

The conservation of mass may be written

$$\rho_{Lj} (4\pi r_j^2) \frac{dr}{dt} \Big|_j = (4\pi r_j^2) \left[\sum_i^K \frac{\xi_i P_i}{(2\pi R_i T)^{1/2}} - \sum_i^K \frac{\xi_i P_{D_j}}{(2\pi R_i T_{D_j})^{1/2}} \right]$$

The droplet pressure is calculated from the Kelvin-Helmholtz expression and is expressed as

$$P_{D_j} = P_{sat,j} \exp \left(\frac{2 m_j \sigma_j}{\rho_j R T r_j} \right)$$

which j indicates properties of the droplet.

If the mass accommodation coefficient ξ_i is defined as zero for all non-condensable species, the droplet growth equation may be put in a more general form as

$$\left. \frac{dr}{dt} \right|_j = \sum_i^n \frac{\xi_i}{\rho_{Lj} (2\pi R_i)^{1/2}} \left[\frac{P_i}{T^{1/2}} - \frac{P_{Dj}}{T_{Dj}^{1/2}} \right] \quad (\text{B.26})$$

where \sum_i^n indicates the summation over all species in the mixture.

Equation (B.26) is valid for the homogeneous growth when $j=1$ and with the definition of ξ_i as being zero until droplet growth (mass accommodation) occurs. Consideration of an energy balance on any droplet of composition j requires the following definition:

$$\alpha_j = \frac{T_{\text{ref},j} - T}{T_{Dj} - T}$$

where α_j is the thermal accommodation coefficient of a droplet j .

The energy flux incident to a droplet j of n total species is

$$(4\pi r_j^2) \sum_i^n \frac{P_i (2R_i T)}{(2\pi R_i T)^{1/2}}$$

The total energy flux reflected from the droplet j is

$$(4\pi r_j^2) \sum_i^n (1 - \xi_i) \frac{P_i (2R_i T_{\text{ref},j})}{(2\pi R_i T)^{1/2}}$$

or

$$(4\pi r_j^2) \sum_i^n (1 - \xi_i) \frac{P_i (2 R_i)}{(2\pi R_i T)^{1/2}} \left[T + \alpha_j (T_{D_j} - T) \right]$$

The total energy evaporated from the droplet j is

$$(4\pi r_j^2) \sum_i^n \frac{\xi_i P_{D_j} (2 R_i T_{D_j})}{(2\pi R_i T_{D_j})^{1/2}}$$

The rate of change of droplet internal energy is

$$\frac{4}{3} \pi r_j^3 \rho_{L_j} C_{P_j} \frac{dT_D}{dt} \Big|_j + 4\pi r_j^2 \frac{dr}{dt} \Big|_j \rho_{L_j} U_{fDI_j}$$

where

$$U_{fDI_j} = h_{fDI_j} = \frac{\gamma_j}{\gamma_j - 1} R_{I_j} T_{D_j} - h_{fgI_j}$$

and C_{P_j} is the specific heat of the liquid drop j .

The conservation of energy therefore requires

$$\begin{aligned} & \frac{4}{3} \pi r_j^3 \rho_{L_j} C_{P_j} \frac{dT_D}{dt} \Big|_j + 4\pi r_j^2 \frac{dr}{dt} \Big|_j \rho_{L_j} \left(\frac{\gamma_j}{\gamma_j - 1} R_{I_j} T_{D_j} - h_{fgI_j} \right) = \\ & (4\pi r_j^2) \left\{ \sum_i^n \frac{P_i (2 R_i T)}{(2\pi R_i T)^{1/2}} - \sum_i^n (1 - \xi_i) \frac{P_i (2 R_i)}{(2\pi R_i T)^{1/2}} \left[T + \alpha_j (T_{D_j} - T) \right] \right. \\ & \left. - \sum_i^n \frac{\xi_i P_{D_j} (2 R_i T_{D_j})}{(2\pi R_i T_{D_j})^{1/2}} \right\} \end{aligned} \quad (B.27)$$

Let

$$\beta_i = \frac{P_i}{T^{1/2}} \quad \text{and} \quad \beta_{D_j} = \frac{P_{D_j}}{T_{D_j}^{1/2}}$$

Equation (B.27) may therefore be reduced to

$$\begin{aligned} & \left. \frac{r_j \rho_{L_j} C_{p_j}}{3} \frac{dT_D}{dt} \right|_j + \rho_{L_j} \left(\frac{\gamma_j}{\gamma_{j-1}} R_{I_j} T_{D_j} - h_{fgI_j} \right) \frac{dr}{dt} \\ & - \sum_i^n \left(\frac{\beta_i (2 R_i T)}{(2 \pi R_i)^{1/2}} - (1 - \xi_i) \frac{\beta_i (2 R_i)}{(2 \pi R_i)^{1/2}} \left[T + \alpha_j (T_{D_j} - T) \right] \right. \\ & \quad \left. - \frac{\xi_i \beta_{D_j} (2 R_i T_{D_j})}{(2 \pi R_i)^{1/2}} \right) = 0 \end{aligned} \quad (\text{B.28})$$

The first term of the left hand side of Eq. (B.28) is shown to be small compared to the second terms in the homogeneous analysis of Duff, Ref. B.4. The term will not be dropped in the mathematical development. It will, however, not be included in the computer solution as the term produces stability problems in the convergence criteria of droplet temperature.

By definition

$$h_{fgI_j} = \lambda_{I_j} C_{pI_j} T = \lambda_{I_j} R_{I_j} T \frac{\gamma_j}{\gamma_{j-1}}$$

also,

$$\left. \frac{dr}{dt} \right|_j = \sum_i^n \frac{\xi_i}{\rho_{L_j} (2 \pi R_i)^{1/2}} \left[\frac{P_i}{T^{1/2}} - \frac{P_{D_j}}{T_{D_j}^{1/2}} \right]$$

The energy equation may be reduced to:

$$\begin{aligned}
 & \frac{r_j \rho_{Lj} C_{pj}}{3} \left. \frac{dT_D}{dt} \right|_j + \rho_{LIj} \left(\frac{\gamma_j}{\gamma_j - 1} R_{Ij} T_{Dj} - h_{fgIj} \right) \sum_i^n \frac{\xi_i}{\rho_{LIj} (2\pi R_i)^{1/2}} (\beta_i - \beta_{Dj}) \\
 & - \sum_i^n \left(\frac{\beta_i (2R_i T)}{(2\pi R_i)^{1/2}} - (1 - \xi_i) \frac{\beta_i (2R_i)}{(2\pi R_i)^{1/2}} \left[T + \alpha_j (T_{Dj} - T) \right] \right. \\
 & \left. - \frac{\xi_i \beta_{Dj} (2R_i T_{Dj})}{(2\pi R_i)^{1/2}} \right) = 0
 \end{aligned} \tag{B.29}$$

or

$$\begin{aligned}
 & \frac{r_j \rho_{Lj} C_{pj}}{3} \left. \frac{dT_D}{dt} \right|_j + \sum_i^n \frac{2 \xi_i \beta_{Dj} R_i}{(2\pi R_i)^{1/2}} T_{Dj} - \sum_i^n \left\{ \beta_i T \sqrt{\frac{2R_i}{\pi}} - (1 - \xi_i) \beta_i \sqrt{\frac{2R_i}{\pi}} T \right. \\
 & \left. - (1 - \xi_i) \beta_i \sqrt{\frac{2R_i}{\pi}} \alpha_j T_{Dj} + (1 - \xi_i) \beta_i \sqrt{\frac{2R_i}{\pi}} \alpha_j T \right. \\
 & \left. + \frac{\xi_i}{\sqrt{2\pi R_i}} (\beta_i - \beta_{Dj}) \left(\frac{\gamma_j}{\gamma_j - 1} \right) R_{Ij} T_{Dj} (\lambda_j - 1) \right\} = 0
 \end{aligned} \tag{B.30}$$

For a noncondensable specie $\xi_i = 0$, therefore, Eq.(B.30) is not carried out to the exact form of a homogeneous droplet analysis by dividing the mass accommodation coefficient. Symbol ξ_i is defined as zero until condensation of specie i occurs in the nozzle. The final form of the energy equation is;

$$\begin{aligned}
& \frac{r_j \rho_{L_j} C_{p_j}}{3} \left. \frac{dT_D}{dt} \right|_j + \sum_i^n \left(\xi_i \beta_{D_j} \sqrt{\frac{2R_i}{\pi}} + (1 - \xi_i) \beta_i \sqrt{\frac{2R_i}{\pi}} \alpha_j \right) T_{D_j} \\
& - \sum_i^n \left\{ \xi_i \beta_i T \sqrt{\frac{2R_i}{\pi}} + (1 - \xi_i) \beta_i \sqrt{\frac{2R_i}{\pi}} \alpha_j T \right. \\
& \left. + \frac{\xi_i}{\sqrt{2\pi R_i}} (\beta_i - \beta_{D_j}) \left(\frac{\gamma_j}{\gamma_j - 1} \right) (\lambda_j - 1) R_{I_j} T_{D_j} \right\} = 0 \quad (B.31)
\end{aligned}$$

Solution of the drop growth equations involves an iteration procedure of T_{D_j} in Eq. (B.31) and the resulting value of the droplet growth rate Eq. (B.26).

Condensation analysis in an expanding flow requires a description of the mass fraction of condensate for all condensable species. The aforementioned quasi-static process used in describing the condensation mechanism necessitates its physical relationship to an expanding flow. This is accomplished by defining the position at which the critical droplet size of the first condensable specie has occurred as in a volume $A(X_1)dX_1$. There are assumed to be m volumes dependent on X , the centerline of the nozzle (see Fig. B-2 for reference).

A mass fraction analysis for each specie involves a separate addition of each specie mass in each quasistatically defined volume. The number of droplets formed in the m^{th} volume $A(X_m)dX_m$ of specie i is,

$$dN_i(X_m) = J_i(X_m) A(X_m) \left[\frac{dX_m}{u} \right] dX_m \quad (B.32)$$

The mass of the newly formed droplets of specie i is

$$M_{ND_i}(X_m) = dN_i(X_m) \rho_{L_i} \left(\frac{4}{3} \pi r_i^{*3} \right) \quad (B.33)$$

The condensed mass rate of specie i on any droplet size with surface area S_j is

$$\sum_j^n \frac{S_j \xi_i P_i}{(2\pi R_i T)^{1/2}}$$

The total evaporated portion of specie i with surface area S_j

$$\sum_j^n \frac{S_j \xi_i P_{D_j}}{(2\pi R_i T_{D_j})^{1/2}}$$

Therefore, the mass growth rate of specie i from volume element X_{m-1} to X_m may be written as

$$\frac{dM_i}{dt} \bigg|_{X_{m-1}}^{X_m} = \sum_{j=1}^{KN} \frac{\xi_i S_j}{(2\pi R_i)^{1/2}} \left[\frac{P_i}{T^{1/2}} - \frac{P_{D_j}}{T_{D_j}^{1/2}} \right] ND_j \quad (B.34)$$

where KN is the number of types of drops in the volume element and ND_j is the number of drops of type j.

The surface area of any droplet j is

$$S_j = 4\pi r_j^2$$

where

$$r_j = r_j \bigg|_{X_{m-1}}^{X_m} + \int_{X_{m-1}}^{X_m} \frac{1}{u} \frac{dr}{dt} \bigg|_j dX$$

Substitution of Eq.(B.32) yields

$$r_j = r_j \Big|_{X_{m-1}} + \int_{X_{m-1}}^{X_m} \frac{ND_j}{u} \sum_i^{KN} \frac{\xi_i}{\rho_{LI_j} (2\pi R_i)^{1/2}} \left[\frac{P_i}{T^{1/2}} - \frac{P_{D_j}}{T_{D_j}^{1/2}} \right] dX_m$$

The surface area therefore becomes

$$S_j = 4\pi \left[r_j \Big|_{X_{m-1}} + \int_{X_{m-1}}^{X_m} \frac{ND_j}{u} \sum_i^{KN} \frac{\xi_i}{\rho_{LI_j} (2\pi R_i)^{1/2}} \left[\frac{P_i}{T^{1/2}} - \frac{P_{D_j}}{T_{D_j}^{1/2}} \right] dX_m \right]^2 \quad (B.35)$$

The total mass of specie i at any volume element is the sum of the mass of the old and new droplets formed in a volume at X_m and the mass growth of all droplets from the volume at X_{m-1} to the volume at X_m . Mathematically,

$$M_i(X_m) = M_{ND_i}(X_m) + M_i(X_{m-1}) + \frac{dM_i}{dt} \Big|_{X_{m-1}}^{X_m} \frac{dX_m}{u}$$

(B.36)

where u defines the freestream velocity.

The total condensed mass of specie i at any volume element is described by Eqs. (B.33), (B.34), (B.35) and (B.36). At the first volume element, e.i., $m = 1$, the last two terms on the right-hand side of Eq. (B.36) are eliminated. Mass growth does not occur until droplets in the preceding volume elements exist.

To obtain the mass fraction of condensed specie i , the continuity equation is defined as

$$\dot{M} = \rho A u$$

where \dot{M} is the total mass flow rate, ρ is the freestream density, A is the effective nozzle area and u is the freestream velocity.

The general form of the mass fraction as a function of nozzle position is

$$\mu_i = \frac{M_i (X_m)}{\dot{M} \frac{dx}{u}} \quad (B.37)$$

REFERENCES

- B.1. Frenkel, J., "Kinetic Theory of Liquids," Oxford University Press, London, 1946.
- B.2. Reiss, H., "Theory of the Liquid Drop Model," Ind. Eng. Chem., Vol. 44, 1952, p.1284.
- B.3. Lothe, J., and G.M. Pound, J. Chem. Phys., Vol. 22, 1942, p.1.
- B.4. Duff, K.M., "Non-Equilibrium Condensation of Carbon Dioxide in Supersonic Nozzles," Report No. 84, Gas Turbine Laboratory, Massachusetts Institute of Technology, Cambridge, Mass., January 1966.
- B.5. Oswatitsch, K., Z. Angew. Math. und Mech., Vol. 22, 1942, p.1.

Appendix C

**DEVELOPMENT OF AXISYMMETRIC/CONDENSATION FLOW
AND CHARACTERISTIC EQUATIONS**

Appendix C

C.1 INTRODUCTION

This appendix presents the axisymmetric flow equations linked with the condensation phenomenon and the resulting characteristic equation to be used in the Method-of-Characteristics Computer Program. The equations were derived with the same assumptions as in the basic one-dimensional flow/condensation analysis. A review of the assumptions is as follows:

- The condensed phase is in the form of a cloud of solid or liquid particles.
- The condensation process consists of homogeneous nucleation and heterogeneous droplet growth.
- Volume occupied by the condensed phase is negligible.
- Each droplet type is assumed to be at a uniform temperature throughout.
- The gaseous and condensed phase are at the same velocity.
- All body forces and electromagnetic forces are neglected.
- Thermal radiation and heat transfer through the nozzle wall are neglected.
- The motion of the condensed phase is ordered and is in the direction of the gas streamline.

Section C.2 of this appendix presents a brief summary of the equations used to derive the axisymmetric flow linked to condensation. Section C.3 presents the characteristic equation for use with the axisymmetric method of characteristics theory. References C-1 to C-4 were used in the derivation.

Nomenclature is the same as in Appendix B unless otherwise noted. The terms u and v are to be defined as the x and r components of velocity, respectively.

C.2 AXISYMMETRIC FLOW/CONDENSATION EQUATIONS

The governing set of equations for the flow of a gas mixture with condensation are written as follows:

Global Continuity Equation

$$\nabla \rho \vec{U} + \sum_i^n \phi_i = 0 \quad (C.2.1)$$

where

$$\phi_i = \nabla \rho_{L_i} \vec{U}$$

Gas Specie Equation

$$\rho \vec{U} \cdot \nabla \alpha_i = \phi_i \quad \left\{ \begin{array}{l} \text{where } \alpha_i = \mu_o - \mu_i \text{ according to the} \\ \text{nomenclature of Appendix B.} \end{array} \right\} \quad (C.2.2)$$

Momentum Equation

$$\rho \vec{U} \cdot \nabla \vec{U} + \nabla P = 0 \quad (C.2.3)$$

Energy Equation

$$\rho \vec{U} \cdot \nabla H - \sum_i^n \rho \vec{U} \cdot \nabla \left\{ L_i + C_{pL_i} \Delta T \right\} = 0 \quad (C.2.4)$$

where

$$\Delta T = T - T_D \quad \text{and} \quad H = h + \frac{1}{2} \vec{U} \cdot \vec{U} \quad (C.2.5)$$

Gas Dynamic Relation

$$T \nabla S = \nabla h - \frac{\nabla P}{\rho} + \sum_i^n \left\{ h_i - T S_i \nabla \alpha_i \right\} \quad (C.2.6)$$

Gas Dynamic Relation Along a Streamline

$$\vec{T}\vec{U} \cdot \nabla S = \vec{U} \cdot \nabla H + \frac{1}{\rho} \sum_i^n \left\{ h_i - TS_i \right\} \alpha_i \quad (C.2.7)$$

Equation of State (in terms of the mixed gases)

$$P = \rho R T \quad (C.2.8)$$

Expanding Eqs. C.2.1 through C.2.8 with use of thermodynamic relationships and vector algebra, one arrives at the combined form

$$\left(1 - \frac{u^2}{a^2}\right) \frac{\partial u}{\partial x} + \left(1 - \frac{v^2}{a^2}\right) \frac{\partial v}{\partial r} - \frac{uv}{a^2} \left(\frac{\partial v}{\partial x} + \frac{\partial u}{\partial r} \right) + \frac{\delta v}{r} - \frac{(\gamma-1)}{a^2} \left(u \frac{\partial H}{\partial x} + v \frac{\partial H}{\partial r} \right) = \frac{B}{a^2} \quad (C.2.9)$$

where

$$a^2 = \gamma R T$$

and

$$B = \left(1 - \frac{(\gamma-1)}{\rho} \sum_i^n (h_i - TS_i) \alpha_i + \frac{a^2}{\rho} \sum_i^n \phi_i \right) \quad (C.2.10)$$

The resulting Eqs. C.2.9 and C.2.10 have been derived in a form compatible with the use of the axisymmetric method of characteristics.

C.3 CHARACTERISTIC SOLUTION OF AXISYMMETRIC FLOW/CONDENSATION EQUATIONS

This section presents the method of characteristics solution for the supersonic flow of a gaseous mixture with condensation. The characteristic solution is obtained by inserting the proper geometric relationships, defining both right- and left-running characteristic waves, as an angular function of streamline direction, into Eq. (C.2.9). This results in

$$\begin{aligned}
 & \left(1 - \frac{u^2}{a^2}\right) \left(\frac{du}{dx} - \beta \frac{\partial u}{\partial r}\right) + \left(1 - \frac{v^2}{a^2}\right) \left(\frac{dv}{dx} - \frac{\partial v}{\partial x}\right) \frac{1}{\beta} - \frac{uv}{a^2} \left(\frac{\partial v}{\partial x} + \frac{\partial u}{\partial r}\right) \\
 & + \frac{\delta v}{r} - \frac{(\gamma-1)}{a^2} \left(u \frac{\partial H}{\partial x} + v \frac{\partial H}{\partial r}\right) = \frac{B}{a^2}
 \end{aligned} \tag{C.3.1}$$

where

$$\beta = \tan(\theta + \mu)$$

The geometry of the system is presented below in Fig. C-1.

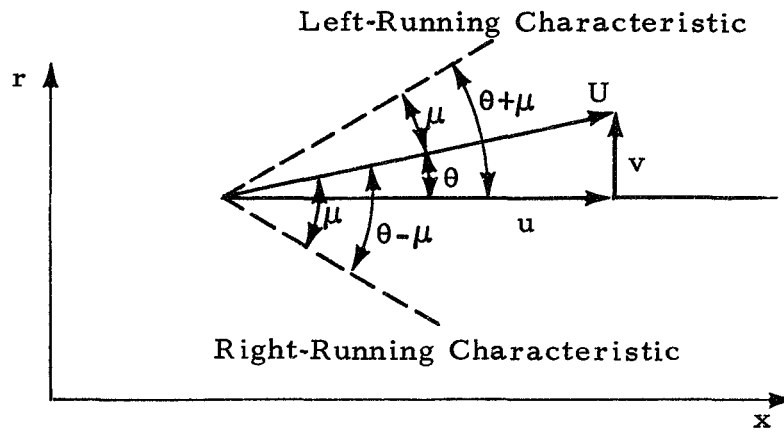


Fig. C-1 - Characteristic Plane

Utilizing the definition of the speed of sound, some vector algebra and introducing the rate of entropy change normal to the streamline, one arrives at

$$\begin{aligned}
 & \left(1 - \frac{u^2}{a^2}\right) \frac{du}{dx} + \frac{1}{\beta} \left(1 - \frac{v^2}{a^2}\right) \frac{dv}{dx} - \left\{ \frac{2uv}{a^2} + \beta \left(1 - \frac{u^2}{a^2}\right) + \frac{1}{\beta} \left(1 - \frac{v^2}{a^2}\right) \right\} \frac{\partial u}{\partial r} \\
 & - \left(\frac{uv}{a^2} + \frac{1}{\beta} \left(1 - \frac{v^2}{a^2}\right) \right) \frac{a^2}{\gamma R U} \frac{\partial S}{\partial n} - \left(\frac{uv}{a^2} + \frac{1}{\beta} \left(1 - \frac{v^2}{a^2}\right) \right) \left\{ \frac{\sin \theta}{U} \left(\sum_i^n (h_i - TS_i) \frac{\partial \alpha_i}{\partial x} \right. \right. \\
 & \left. \left. + \frac{\partial H}{\partial x} \right) - \frac{\cos \theta}{U} \left(\sum_i^n (h_i - TS_i) \frac{\partial \alpha_i}{\partial r} + \frac{\partial H}{\partial r} \right) \right\} - \frac{(\gamma-1)}{a^2} \left(u \frac{\partial H}{\partial x} + v \frac{\partial H}{\partial r} \right) + \frac{\delta v}{r} = \frac{B}{a^2}
 \end{aligned} \tag{C.3.2}$$

At this point, a β is found for which the coefficient $\partial u / \partial r$ is zero. This results in

$$\beta = \frac{-\frac{uv}{a^2} \pm \sqrt{\frac{U^2}{a^2} - 1}}{1 - \frac{u^2}{a^2}} \quad (C.3.3)$$

With further substitutions, Eq. (C.3.2) can be reduced to an exact differential. Small terms which arise due to condensation are neglected and the final form of the characteristic solution is

$$\boxed{\begin{aligned} d\theta \pm \cot\mu \frac{dU}{U} \mp \frac{\sin\mu \cos\mu}{\gamma RT} \left(\frac{dP}{\rho} + U dU \right) \\ \pm dH \frac{\sin\mu \cos\mu}{\gamma RT} \mp \delta \frac{\sin\mu \sin\theta}{\sin(\theta \mp \mu)} \frac{dr}{r} = 0 \end{aligned}} \quad (C.3.4)$$

The characteristics equation derived for the axisymmetric flow condition without condensation effects is identical to Eq. (C.3.4) with the exception of the enthalpy term, dH . The fact that condensation effects show up as an additive term indicates a simpler computer program solution than originally anticipated using the present MOC program.

REFERENCES

- C.1 Migdal, D., and V. D. Agosta, "Supersonic Gas-Particle Flow with Chemical Reactions," Phys. Fluids, Vol. 10, No. 4, April 1967.
- C.2 Hoffman, J. D., "An Analysis of the Effects of Gas-Particle Mixtures on the Performance of Rocket Nozzles," Report No. TM-63-1 (JPC 348), Purdue University, West Lafayette, Ind., January 1963.
- C.3 Penny, M. M., "Final Report — Analysis of Base Heating Data from Solid Strap-On Tests; Vol. II, A Method-of-Characteristics Solution for the Supersonic Flow of a Gas-Particle Mixture," LMSC/HREC A791268-II, Lockheed Missiles & Space Company, Huntsville, Ala., March 1968.
- C.4 Edelman, R., et al., "Generalized Viscous Multicomponent-Multiphase Flow with Application to Laminar and Turbulent Jets of Hydrogen," GASL TR 349, General Applied Sciences Laboratories, Westbury, N. Y., June 1963.